



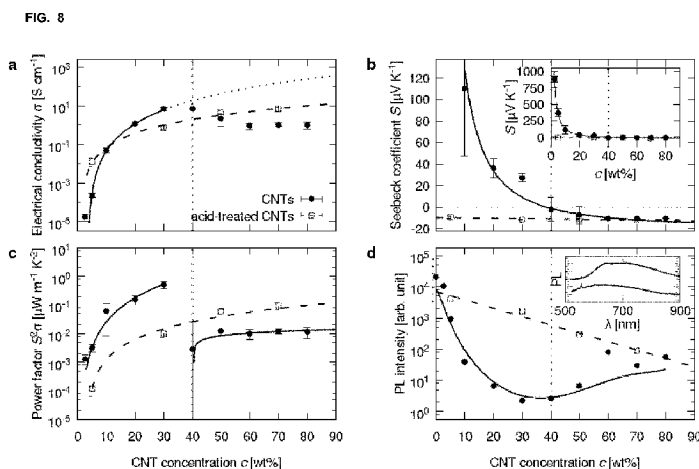
- (51) International Patent Classification:
H01L 51/00 (2006.01)
- (21) International Application Number:
PCT/EP2016/078459
- (22) International Filing Date:
22 November 2016 (22.11.2016)
- (25) Filing Language: English
- (26) Publication Language: English
- (30) Priority Data:
P201531706 24 November 2015 (24.11.2015) ES
- (71) Applicant: CONSEJO SUPERIOR DE INVESTIGACIONES CIENTIFICAS (CSIC) [ES/ES]; C/ Serrano, 117, 28006 Madrid (ES).
- (72) Inventors: CAMPOY QUILES, Mariano; Instituto De Ciencia De Materiales De Barcelona (icmab), Campus Universidad Autonoma De Barcelona (bellaterra), 08193 Cerdanyola del Vallès (Barcelona) (ES). GOÑI TASADA, Alejandro Rodolfo; Instituto De Ciencia De Materiales De Barcelona (icmab), Campus Universidad Autonoma De Barcelona (bellaterra), 08193 Cerdanyola del Vallès (Barcelona) (ES). DÖRLING, Bernhard; Instituto De Ciencia De Materiales De Barcelona (icmab), Campus Universidad Autonoma De Barcelona (bellaterra), 08193 Cerdanyola del Vallès (Barcelona) (ES). MÜLLER, Christian; CHALMERS UNIVERSITY OF TECHNOLOGY, Polymer Technology, SE-412 96 Gothenburg (SE). RYAN,

Jason; University of Kentucky, Center for Applied Energy Research, 2540 Research Park Drive, Lexington, Kentucky 40511 (US).

- (74) Agent: PONS ARIÑO, Ángel; Glorieta de Rubén Darío, 4, 28010 Madrid (ES).
- (81) Designated States (unless otherwise indicated, for every kind of national protection available): AE, AG, AL, AM, AO, AT, AU, AZ, BA, BB, BG, BH, BN, BR, BW, BY, BZ, CA, CH, CL, CN, CO, CR, CU, CZ, DE, DJ, DK, DM, DO, DZ, EC, EE, EG, ES, FI, GB, GD, GE, GH, GM, GT, HN, HR, HU, ID, IL, IN, IR, IS, JP, KE, KG, KN, KP, KR, KW, KZ, LA, LC, LK, LR, LS, LU, LY, MA, MD, ME, MG, MK, MN, MW, MX, MY, MZ, NA, NG, NI, NO, NZ, OM, PA, PE, PG, PH, PL, PT, QA, RO, RS, RU, RW, SA, SC, SD, SE, SG, SK, SL, SM, ST, SV, SY, TH, TJ, TM, TN, TR, TT, TZ, UA, UG, US, UZ, VC, VN, ZA, ZM, ZW.
- (84) Designated States (unless otherwise indicated, for every kind of regional protection available): ARIPO (BW, GH, GM, KE, LR, LS, MW, MZ, NA, RW, SD, SL, ST, SZ, TZ, UG, ZM, ZW), Eurasian (AM, AZ, BY, KG, KZ, RU, TJ, TM), European (AL, AT, BE, BG, CH, CY, CZ, DE, DK, EE, ES, FI, FR, GB, GR, HR, HU, IE, IS, IT, LT, LU, LV, MC, MK, MT, NL, NO, PL, PT, RO, RS, SE, SI, SK, SM, TR), OAPI (BF, BJ, CF, CG, CI, CM, GA, GN, GQ, GW, KM, ML, MR, NE, SN, TD, TG).

Published:
— with international search report (Art. 21(3))

(54) Title: A PROCESS OF OBTAINMENT OF AN N-TYPE OR A P-TYPE ORGANIC SEMICONDUCTOR BY UV-VIS IRRADIATION



(57) Abstract: The invention relates to a process of obtainment of an n-type or a p-type organic semiconductor by irradiating a p-type or an n-type organic semiconductor with UV-VIS radiation, respectively.

WO 2017/089351 A1

**A PROCESS OF OBTAINMENT OF AN N-TYPE OR A P-TYPE ORGANIC
SEMICONDUCTOR BY UV-VIS IRRADIATION**

DESCRIPTION

5

The invention relates to a process of obtainment of an n-type or a p-type organic semiconductor by irradiating a p-type or an n-type organic semiconductor with UV-VIS radiation, respectively.

10 **STATE OF ART**

A broad range of organic electronic applications rely on the availability of both p- and n-type organic semiconductors, and the possibility to deposit them as sequential layers or to form spatial patterns. Examples include transport layers in diodes (OLEDs, photovoltaics, etc), the transistor technology that underpins complementary logic and circuitry, as well as the p- and n- legs of a thermoelectric generator. Typically, a judicious selection of orthogonal solvents coupled to additive patterning techniques, such as inkjet printing, is employed to provide patterned p- and n- regions in solution-processed devices. If higher resolution is required (below ~100 μm), multi-step lithographic methods are then compulsory.

Besides inkjet printing, organic thermoelectric generators are prepared using a variety of methods, including drop casting, spray coating or (vacuum) filtering the solution, to obtain single layers, and subsequently assembling the complete device. In all these cases, the n-type character is obtained by either molecular doping of the organic semiconductor, or by forming composites with n-type fillers, such as nitrogen doped carbon nanotubes.

Furthermore, organic n-type materials in particular prove difficult to handle, due to their inherent chemical instability towards oxidation in air, since their LUMO is normally located about 3 eV below the vacuum level, To circumvent this, a variety of strategies have been employed, like doping with air-stable intermediate compounds or by efforts to synthesize compounds with a precisely controlled LUMO level.

35

DESCRIPTION OF THE INVENTION

It can be found in the state of the art, that fabrication processes of n- or p-type semiconducting devices usually require the deposition of both, n- and p-type materials.

5 In the present invention only one solution of a p-type material has to be deposited and subsequently irradiated with light. Therefore, the present invention significantly simplifies the fabrication process of such kind of devices.

10 Because the deposition itself comprises only a single step, this automatically ensures good electrical as well as physical contact between n- and p- regions, thereby minimizing contact resistance and avoiding dewetting and delamination issues. All of this allows to reduce the minimum process complexity, by not only forgoing the deposition step for the complementary semiconductor layer, but also potentially avoiding the need for further deposition steps of metallic interconnect layers in some
15 devices like thermoelectric generators.

When depositing complex multilayer structures from solution, a careful selection of orthogonal solvents is necessary, so as not to damage any of the exposed, underlying layers. Being able to prepare a similar structure with less deposition steps immediately
20 relaxes requirements further, or if desired, instead allows for even more complex structures without additional cost.

The procedure also helps to obtain a higher thickness homogeneity compared to additive manufacturing.

25

Because the patterning is done with light, the resolution of the p- and n- regions can be increased from around 50 μm for state-of-the-art inkjet printed features, down to 1 μm for a standard photolithographic step.

30 Unlike prevailing n-type organic materials, which often cannot be processed or operated in atmosphere, the materials related to this invention are stable in air over weeks and months, as was demonstrated by preparing, operating and storing them in atmosphere.

A first aspect of the present invention relates to a process of obtainment of an n-type organic semiconductor or a p-type organic semiconductor characterized in that the process comprises the following steps:

5 a) preparing a film of a p-type organic semiconductor or an n-type organic semiconductor onto a substrate respectively,

wherein the organic semiconductor comprises a semiconducting nanostructure and an acceptor or donor of electrons respectively; and

10 b) irradiating the film obtained in step (a) by UV-VIS radiation with a power between 1 mW/cm² and 100 mW/cm² and an exposure time of between 0.1 s and 600 s.

In a preferred embodiment, the invention relates to a process of obtainment of an n-type organic semiconductor characterized in that the process comprises the following steps:

15 a) preparing a film of a p-type organic semiconductor onto a substrate;

wherein said p-type organic semiconductor comprises

- an n-type semiconducting nanostructure ranging a weight percent between 0.1 % and 60 %, preferably a weight percent between 20 % and 40 %; and
- 20 • a p-type semiconducting conjugated molecule as an acceptor of electrons;

and wherein said n-type organic semiconductor nanostructure is dispersed into the p-type semiconducting conjugated molecule; and

25 b) irradiating the film obtained in step (a) by UV-VIS radiation with a power between 1 mW/cm² and 100 mW/cm² and an exposure time of between 0.1 s and 600 s, preferably with a power between 40 mW/cm² and 60 mW/cm² and an exposure time between 50 s and 100 s.

30 The process of the invention starts with the preparation of a film of a p-type organic semiconductor which comprises

- an n-type semiconducting nanostructure ranging a weight percent between 0.1 % and 60 %; preferably a weight percent between 20 % and 40 %; and

35

- a p-type semiconducting conjugated molecule;

and wherein the n-type semiconducting nanostructure is dispersed into the p-type semiconducting conjugated molecule;

5

In semiconductors, electrical conduction is explained in terms of majority and minority carriers of electric charge. In n-type semiconductor materials, electrons are the majority carriers and holes, i.e. the vacancies left by electrons, are the minority carriers. In p-type semiconductor materials the opposite is true: the holes are the majority carriers and the electrons are the minority carriers. The carrier type can be determined experimentally using for example the Seebeck effect or the Hall effect.

In the present invention, the terms “n-type organic semiconductor and p-type organic semiconductor” are used inclusively, and refer to an n-type semiconductor and a p-type organic semiconductor, respectively, comprising at least one organic component. It is not meant to exclude further, inorganic components.

The term “n-type semiconducting nanostructure” refers herein to a material having at least one dimension below a length of 100 nm, for instance nano-scale particles, wires, rods, tubes, fibres, ribbons, sheets or platelets which exhibit n-type semiconductivity.

Preferred examples of n-type semiconducting nanostructures are N-doped carbon nanotubes, N-doped graphene sheets and graphite nanoplatelets, N-doped graphene nanoribbons, fullerenes, phosphorus doped silicon nanowires, tellurium based nanowires such as Bi_2Te_3 nanowires or PbTe nanowires), zinc oxide based nanowires, titanium oxide based nanowires, and a combination thereof.

The term “p-type semiconducting conjugated organic molecule” refers herein to conjugated polymers or conjugated small molecules i.e. organic molecules which contain extended systems of delocalized π -electrons which exhibit p-type semiconductivity. It also includes subgroups such as polyelectrolytes and donor-acceptor polymers.

Examples for p-type semiconducting conjugated organic molecules are polyalkylthiophenes, polyfluorenes, polyaniline (PANI), polyacetylene, polyphenylene

vinylene (PPV), tetracyanoquinodimethane, tetrathiafulvalene, and a combination thereof. Poly(3-hexylthiophene) (P3HT), poly(3-dodecylthiophene-2,5-diyl) (P3DDT) or poly(9,9-dioctylfluorene) are preferred.

5 In the p-type organic semiconductor of the present invention, the n-type semiconducting nanostructure is dispersed into the p-type semiconducting conjugated molecule so that the n-type semiconducting nanostructure percolates throughout the p-type semiconducting conjugated molecule. Percolation of the n-type semiconducting nanostructure throughout the p-type semiconducting conjugated molecule starts at a
10 weight percent (percolation concentration) of around 0.1 %; depends, for example on the length of the nanotubes and the degree of aggregation. For well dispersed and very long CNT, percolation may be obtained for really low concentrations of CNT, close to 0.1 %. In a preferred embodiment of the process of the invention, the n-type semiconducting nanostructure ranges a weight percent between 20 % and 40 %.

15

Step (a) of the preferred process of the invention refers to the preparation of a film of a p-type organic semiconductor onto a substrate.

Substrates could be rigid or flexible.

20

Substrates can be consisting of a glass, a ceramic, a metal, wood, a polymer such as a rubber, a mineral, concrete, a cellulosic material, a textile such as cotton, linen, nylon, silk, velvet and leather or biological tissues such as skin.

25 Preferred examples of substrates are flexible substrates selected from polyethylene terephthalate (PET), polyethylene naphthalate (PEN), polyimide, polyethylene (PE), polystyrene (PS), poly(vinyl chloride) (PVC), polytetrafluoroethylene (PTFE, Teflon), polypropylene (PP), polyurethane (PU), polyvinylidene fluoride (PVDF) and a combination thereof.

30

In a preferred embodiment of the process of the invention, the preparation of a film of a p-type organic semiconductor onto a substrate, this is step (a) of the process, comprises the following steps:

a1) adding a solution of a p-type semiconducting conjugated molecule comprising a p-type semiconducting conjugated molecule and a solvent to an n-type semiconducting nanostructure dispersion comprising an n-type semiconducting nanostructure and a solvent;

5

a2) agitating the mixture obtained in (a1) at a temperature range between -20 °C and 200 °C; preferably at a temperature range between 0 °C and 100 °C,

a3) depositing the solution obtained in step (a2) onto a substrate.

10

In step (a1), the p-type semiconducting conjugated molecule solution comprises a p-type semiconducting conjugated molecule as defined above, and a solvent. Examples of solvents are chlorobenzene, 1,2-dichlorobenzene, 1,4-dichlorobenzene, 1,2,4-trichlorobenzene, chloroform, toluene, o-xylene, p-xylene, water, methanol, ethanol and isopropanol.

15

In step (a1), the n-type semiconducting nanostructure dispersion comprises an n-type semiconducting nanostructure as described above and a solvent. Examples of solvents are chlorobenzene, 1,2-dichlorobenzene, 1,4-dichlorobenzene, 1,2,4-trichlorobenzene, chloroform, toluene, o-xylene, p-xylene, water, methanol, ethanol and isopropanol.

20

Step (a1) refers to the addition of a p-type semiconducting conjugated molecule solution to an n-type semiconducting nanostructure dispersion.

25 Step (a2) refers to the agitation of the mixture obtained in (a1) at a temperature range between -20 °C and 200°C, preferably between 0 °C and 100 °C. Agitation, such as sonication, is necessary to debundle the n-type semiconducting nanostructures.

Step (a3) relates to the deposition of the solution obtained in step (a3) onto a substrate. Possible substrates are defined above. Preferred deposition techniques are drop casting, filtering, dip coating, blade coating, slot-die coating, spray coating, bar coating, screen printing, gravure printing, flexographic printing or inkjet printing.

30

In a preferred embodiment, the process of the invention comprises a step (a1'), between step (a1) and step (a2), of adding a surfactant to the mixture obtained in (a1). The surfactant may help to debundle the n-type semiconducting nanostructures.

- 5 A wet film is obtained after step (a3); in this preferred embodiment of the process of the invention, step (b), i.e. the irradiation with UV-VIS radiation, is performed while the film is wet.

Preferably, the wet film obtained in step (a) has a thickness between 10 μm and 1000 μm , more preferably between 100 μm and 1000 μm .

In another preferred embodiment of the process of the invention, step (a) comprises the following steps:

- 15 steps (a1) to (a3) as described above, i.e. (a1) adding a p-type semiconducting conjugated molecule solution comprising a p-type semiconducting conjugated molecule and a solvent to an n-type semiconducting nanostructure dispersion comprising an n-type semiconducting nanostructure and a solvent; (a2) agitating the mixture obtained in (a1) at a temperature range between -20°C and 200°C , preferably between 0°C and 100°C , and (a3) depositing the solution obtained in step (a2) onto a substrate;

and

- 25 a step (a4) of drying the wet film obtained in step (a3) by evaporating the solvents.

A dried film is obtained after step (a4); this preferred embodiment of the process of the invention relates to the irradiation of the dried film with UV-VIS radiation.

30

In a preferred embodiment, the obtained dried film has a thickness between 10 nm and 100 μm . Preferably, the dried film obtained in step (a) has a thickness between 1 μm and 10 μm .

Another preferred embodiment of the invention relates to a process of obtainment of a p-type organic semiconductor as described above, characterized in that the process comprises the following steps:

a) preparing a film of an n-type organic semiconductor onto a substrate

5 wherein said n-type organic semiconductor comprises

- a p-type semiconducting nanostructure ranging a weight percent between 0.1 % and 80 %; and
- an electron-rich molecule as a donor of electrons;

10 and wherein said p-type semiconducting nanostructure is dispersed into the electron-rich molecule; and

b) irradiating the film obtained in step (a) by UV-VIS radiation with a power between 1 mW/cm² and 100 mW/cm² and an exposure time of between 0.1 s and 600 s.

15 The term “p-type semiconducting nanostructure” refers herein to a material having at least one dimension below a length of 100 nm, for instance nano-scale particles, wires, rods, tubes, fibres, ribbons, sheets or platelets which exhibit p-type semiconductivity.

20 Preferred examples of p-type semiconducting nanostructures are pristine single-double- and multi-walled carbon nanotubes, graphene sheets and graphite nanoplatelets, graphene nanoribbons; boron doped single- double- and multi-walled carbon nanotubes, boron doped graphene sheets and boron doped graphite nanoplatelets, boron doped graphene nanoribbons, boron doped fullerenes; boron doped silicon nanowires and a combination thereof

25 The term “electron-rich molecule” refers herein to n-type conjugated small molecules, n-type conjugated polymers, and other molecules that have the capacity to n-dope the p-type semiconducting nanostructure.

30 Preferred examples of electron-rich molecules used in the present invention are polyethylenimine (PEI), diethylenetriamine (DETA), tetramethylammonium hydroxide (TMAH), tetrakis(dimethylamino)ethylene (TDAE), 4-*H*-benzimidazol-2-yl)-*N,N*-dimethylbenzenamine (N-DMBI), 4-*H-N,N*-diphenylaniline (N-DPBI), triphenylphosphine (tpp), 1,3-bis(diphenylphosphino)propane (dppp).

In the n-type organic semiconductor of the present invention, the p-type semiconducting nanostructure is dispersed into the electron-rich molecule so that the p-type semiconducting nanostructure percolates throughout the electron-rich molecule.

5 Step (a) of the preferred process of the invention refers to the preparation of a film of an n-type organic semiconductor onto a substrate. Preferably, the p-type semiconducting nanostructure of step (a) ranges a weight percent between 40 % and 80 %.

10 Substrates could be rigid or flexible.

Substrates can be consisting of a glass, a ceramic, a metal, wood, a polymer such as a rubber, a mineral, concrete, a cellulosic material, a textile such as cotton, linen, nylon, silk, velvet and leather or biological tissues such as skin.

15

Preferred examples of substrates are flexible substrates selected from polyethylene terephthalate (PET), polyethylene naphthalate (PEN), polyimide, polyethylene (PE), polystyrene (PS), poly(vinyl chloride) (PVC), polytetrafluoroethylene (PTFE, Teflon), polypropylene (PP), polyurethane (PU), polyvinylidene fluoride (PVDF) and a
20 combination thereof.

In the present invention, the term "UV-VIS radiation" refers to a wavelength range of between 100 nm to 800 nm. UV radiation regarding a wavelength range of between 200 nm and 350 nm is preferred.

25

In a preferred embodiment, step (b) is performed in the presence of an oxygen containing atmosphere. UV light of wavelength up to ~ 250 nm is mostly absorbed by oxygen O₂ so that ozone O₃ is produced.

30 The irradiation of step (b) is performed using a laser source, a diode or a lamp. Preferably, UV-VIS irradiation is performed using a lamp.

The wet or the dried film can be partially or completely exposed to UV-VIS radiation. A mask is preferably used for partially exposition of the wet or dried film to UV-VIS
35 radiation.

UV-VIS irradiation of the films can be performed by

- rotatory movement of the UV irradiation source, i. e. including the irradiation from all angular directions; 90° irradiation (perpendicular to the film) is preferred; and
- a vertical and horizontal movement of the film

The n-type or p-type organic semiconductor obtained by the process of the invention can be used as part of an electric or electronic device.

Furthermore, the n-type or p-type organic semiconductor obtained by the process of the invention can be used as part of a thermoelectric generator.

Unless otherwise defined, all technical and scientific terms used herein have the same meaning as commonly understood by one of ordinary skilled in the art to which this invention belongs. Methods and materials similar or equivalent to those described herein can be used in the practice of the present invention. Throughout the description and claims the word "comprise" and its variations are not intended to exclude other technical features, additives, components, or steps. Additional objects, advantages and features of the invention will become apparent to those skilled in the art upon examination of the description or may be learned by practice of the invention. The following examples and drawings are provided by way of illustration and are not intended to be limiting of the present invention.

BRIEF DESCRIPTION OF THE DRAWINGS

Figure 1. Scanning electron micrographs of the nanostructure of four representative CNT/P3HT nanocomposites (from top left to bottom right: 30 wt% CNTs, 80 wt% CNTs, 30 wt% acid-treated CNTs, and 60s UV-treated 30 wt% CNTs). Varying amounts of CNT bundles and P3HT matrix are visible in all samples. Additionally, the 80 wt% samples contain Fe-catalyst, and in the UV-treated samples, scrap-like features are visible.

Figure 2. AFM topography of the four representative CNT/P3HT nanocomposites (from top left to bottom right: 30 wt% CNTs, 80 wt% CNTs, 30 wt% acid-treated CNTs, and 60s UV-treated 30 wt% CNTs) shows that 80 wt% and UV-treated samples exhibit considerable roughness.

5

Figure 3. Transmission X-ray micrograph measured at 399 eV, slightly above K_{α} (nitrogen). Darker areas correspond to increased absorption, due to the presence of nitrogen.

10 **Figure 4.** Transmission X-ray micrograph measured at 520 eV. Darker areas correspond to increased absorption not specific to any element. They are instead indicative of increased sample thickness.

Figure 5. Transmission X-ray micrograph measured at 707 eV, slightly above L_{α} (iron).
15 Darker areas correspond to increased absorption caused by iron in the sample.

Figure 6. Conductive AFM measurements of the four representative CNT/P3HT nanocomposites (from top left to bottom right: 30 wt% CNTs, 80 wt% CNTs, 30 wt% acid-treated CNTs, and 60s UV-treated 30 wt% CNTs).. The scale is proportional to the
20 logarithm of the measured current.

Figure 7. Histograms of the conductive AFM measurements of the four representative CNT/P3HT nanocomposites (from top left to bottom right: 30 wt% CNTs, 80 wt% CNTs, 30 wt% acid-treated CNTs, and 60s UV-treated 30 wt% CNTs). We relate the four main
25 peaks to degraded P3HT (a), P3HT of increasing degree of doping (b, c), and CNTs (d).

Figure 8. Dependence of thermoelectric properties on CNT concentration for as synthesized (filled circles, solid line) and acid-treated CNTs (open squares, dashed
30 line).

Figure 9. Photograph of a first proof of concept device made from five pairs of legs made from 20 wt% and 80 wt% composites on PET substrate. The device delivers a Seebeck voltage of $\sim 170 \mu\text{V/K}$.

35

Figure 10. Sample properties after UV-irradiation during deposition.

(a) Seebeck coefficient versus UV treatment duration for samples containing 20 wt% CNTs (open triangles) and 30 wt% CNTs (filled circles). The lines serve as a guide to the eye. The error bars represent the standard deviation.

5 (b) Normalized absorbance (dot-dashed lines) and PL spectra (solid lines) of 20 wt% CNT samples that have been irradiated for extraneous amounts of time.

Figure 11. Optical micrographs of as prepared 30 wt% CNT composite (a), and after 60s (b), 150s(c), and 240s (d) of UV irradiation. The scale bar is 200 μm .

10

Figure 12. Raman spectra of 30 wt% CNT samples before (open circles) and after 60s UV irradiation (open squares), and for a 70wt% CNT sample (open triangles). We relate the marked peaks around 1300 cm^{-1} and 1600 cm^{-1} to the D- and the G-band of the CNTs, and the peak at around 1450 cm^{-1} to the symmetric C=C stretching mode of P3HT.

15

Figure 13. Dependence of electrical conductivity on UV-treatment duration for 20 wt% (open triangles) and 30 wt% samples (filled circles). The error bars represent the standard deviation.

20

Figure 14. FTIR spectra measured by attenuated total reflectance (ATR) infrared spectroscopy of P3HT solutions that have been UV-treated for different amounts of time (a, b) and a summary of relative peak heights plotted versus time (c)

25 **Figure 15.** Proposed fabrication and applications of a device geometry that plays on the advantages of the presented material. The different layers are denoted as substrate (s), electrically conducting interconnect (c), wet film of p-type solution (p1), wet film of UV-treated solution (n1), dried p-type film (p2), dried n-type film (n2).

30 **Figure 16.** Output current (open symbols) and output power (filled symbols) for the device with 15 pairs of legs shown in Figure 14.

Figure 17. Stability of the electrical conductivity σ (open symbols) and the Seebeck coefficient S (filled symbols) over time.

35

Figure 18. Seebeck coefficient of composites of single-walled CNTs (which are p-type due to doping with atmospheric oxygen), n-doped with electron-rich PEI.

EXAMPLES

5

Example 1: Preparation of an n-type organic semiconductor

Preparation of CNT/P3HT composites

10 *Materials:*

Nitrogen doped multi-walled carbon nanotubes were synthesized from a saturated solution of acetonitrile/ferrocene feedstock by chemical vapour deposition (CVD). CNTs contain approximately 7 wt% nitrogen, as determined by EELS/STEM analysis.

15

Poly(3-hexylthiophene-2,5-diyl) (P3HT, $M_w \sim 97 \text{ kg mol}^{-1}$, $M_w/M_n \sim 2.4$, regioregularity > 90%), ortho-dichlorobenzene (oDCB) (99% ReagentPlus) and chloroform (> 99.9% CHROMASOLV) were obtained from Sigma Aldrich.

20 *Sample preparation.*

CNTs were dispersed in oDCB at a concentration of 1 gL^{-1} and sonicated in ice water for 60 min (JP Selecta Ultrasons 50W). P3HT was dissolved in chloroform at a concentration of 20 gL^{-1} and an appropriate amount was added in three steps to the
25 CNT dispersion, to create a mixture with the desired CNT concentration. After each addition, the mixture was sonicated an additional 30 min in ice water. After a day, a precipitate of undissolved, residual carbon and sedimented CNTs, can be observed, the remaining solution was stable for months.

30 1.5 ml of solution was drop-cast onto PET substrates and left to evaporate. Some samples were irradiated with 50 mWcm^{-2} of UV-light directly after solution deposition in a Jelight UVO-Cleaner 42.

Characterization of CNT/P3HT composites

Techniques:

5 *Electrical characterization.* The Seebeck coefficient was measured at 300 K and ambient atmosphere with an SB1000 instrument equipped with a K2000 temperature controller from MMR Technologies using a thermal load of about 1-2 K and a constantan wire as an internal reference. For each composition, six 5 mm by 1 mm small samples from two independently prepared films were measured; each
10 measurement was repeated 10 times. Samples were contacted with silver paste from Agar Scientific.

The electrical conductivity measurements were performed on separate samples from the same batch. Four silver paste contacts were placed in the corners of the 1cm by
15 1cm samples. Conductivity was measured with an Ecopia HMS-5000 Hall measurement system, using the van der Pauw method.

Bulk thermal conductivity. Samples for thermal conductivity measurements were prepared by (1) solidifying material from combined 1 gL⁻¹ CNTs in ODCB and 20 gL⁻¹
20 P3HT in CHCl₃ solutions, (2) compacting material at ambient temperature and a pressure of 18.5 kNcm⁻² to form two identical round pellets with a diameter of 13 mm, and (3) hot-pressing pellets at 150 °C at a pressure of less than 7.4 kNcm⁻². The density was estimated by measuring the volume and weight of the pellets. The heat capacity and thermal diffusivity were measured at ambient temperature with a TPS
25 2500 S piece of equipment from Hotdisk AB using an isotropic model.

Physical characterization. Sample thickness was measured using a KLA Tencor MicroXAM-100 optical surface profilometer for samples with 50 wt% CNTs and below. Samples with higher CNT concentration were measured using a KLA Tencor P16+
30 profilometer. Sample thickness ranged between 15 μm and 0.8 μm, depending on the total solution concentration. For high CNT wt% composites, the samples contain a significant amount of voids, and consequently the total amount of material is overestimated.

Optical characterization. Transmission spectra of samples were measured using a GES-5E ellipsometer from Sopralab. Raman and photoluminescence spectra were measured in backscattering configuration with a LabRam HR800 spectrometer (Horiba JobinYvon) coupled to a confocal Olympus microscope, using 514 nm and 633 nm
 5 excitation wavelengths. Optical micrographs were taken using an Olympus BX51 optical microscope and a DP20 microscope digital camera.

Structural characterization. Scanning electron microscopy was conducted using a FEI Quanta 200 FEG. Atomic Force Microscopy (AFM) and Current sensing AFM were
 10 measured using an Agilent 5500LS instrument with a Rocky Mountain Nanotechnology solid platinum tip. TXM was conducted at the MISTRAL beamline at the ALBA synchrotron. For this, samples were drop-cast onto copper grids.

Results

15

Composites with different stoichiometries, and post-treatments were prepared. Table 1 shows the compositions and treatments applied to each composite.

Table 1:

20

Composites
2.5; 5; 10; 20; 30; 40; 50; 60; 70; 80 wt% CNTs
5; 30; 50; 70 wt% acid-treated CNTs
20 wt% composites UV irradiated for 20, 40, 60, 80 seconds 30 wt% composites UV irradiated for 10, 20, 30, 40, 50 60, 70, 80, 90, 120, 150, and 240 seconds

Four representative CNT/P3HT composites were selected and are summarized in Table 2.

25 Table 2: Representative CNT/P3HT composites:

(a) 30 wt% CNTs	(b) 80 wt% CNTs
(c) 30 wt % acid treated CNTs	(d) 30 wt% CNTs 60s UV-treated

Figure 1 shows the Scanning electron micrographs of the nanostructure of four representative CNT/P3HT nanocomposites given in Table 2 (from top left to bottom right: (a) 30 wt% CNTs, (b) 80 wt% CNTs, (c) 30 wt% acid-treated CNTs, and (d) 60s UV-treated 30 wt% CNTs). Varying amounts of CNT bundles and P3HT matrix are visible in all samples. Additionally, the 80 wt% samples contain Fe-catalyst, and in the UV-treated samples, scrap-like features are visible.

Scanning electron microscopy (SEM) images of composites of P3HT and nitrogen doped multi-walled CNTs with low CNT content ($c \sim 30$ wt%) appear well dispersed, while high CNT content samples ($c \sim 80$ wt% CNTs) exhibit agglomeration (Figure 1a). In all cases, we observe thick fibrillar structures with a diameter of 90 ± 30 nm, which are likely CNT bundles wrapped with polymer.

Figure 2 shows AFM topography of the four representative CNT/P3HT nanocomposites (from top left to bottom right: 30 wt% CNTs, 80 wt% CNTs, 30 wt% acid-treated CNTs, and 60s UV-treated 30 wt% CNTs) shows that 80 wt% and UV-treated samples exhibit considerable roughness.

Moreover, Atomic force microscopy (AFM) images reveal an increase in surface roughness with increasing CNT content (Figure 2). The resulting films clearly show a fine fibrillar structure with an average bundle diameter of 55 ± 15 nm, which is significantly smaller than for the high CNT content samples (Figure 1 and 2).

Figure 3, 4 and 5 shows Transmission X-ray micrographs measured at 399 eV, 520 eV and 707 eV, respectively. The measurements depicted in Figure 3 are slightly above K_{α} (nitrogen). Darker areas correspond to increased absorption, due to the presence of nitrogen. Darker areas shown in Figure 4 correspond to increased absorption not specific to any element. They are instead indicative of increased sample thickness. The measurements depicted in Figure 5 are slightly above L_{α} (iron). Darker areas correspond to increased absorption caused by iron in the sample.

We employed transmission X-ray microscopy (TXM) to confirm that the CNTs are distributed homogeneously all throughout the thickness of the film, as well as on the

surface (Figure 3, 4 and 5). TXM also reveals the presence of iron-rich clusters in the sample, that is, residuals from the CNT synthesis

Figure 6 shows the Conductive AFM measurements of the four representative
5 CNT/P3HT nanocomposites (from top left to bottom right: 30 wt% CNTs, 80 wt% CNTs, 30 wt% acid-treated CNTs, and 60s UV-treated 30 wt% CNTs) and Figure 7 the histograms of said conductive AFM measurements. The four main peaks are related to degraded P3HT (a), P3HT of increasing degree of doping (b, c), and CNTs (d). Electrically, the composites consist of highly conductive, CNT-rich regions surrounded
10 by polymer-rich regions that exhibit *circa* four orders of magnitude lower electrical conductivity (Figure 6 and 7).

Figure 8 shows the dependence of thermoelectric properties on CNT concentration for
15 as synthesized (filled circles, solid line) and acid-treated CNTs (open squares, dashed line).

(a) The electrical conductivity σ shows percolative behavior, increasing by several orders of magnitude upon addition of a few wt% of CNTs. At high CNT content, a dip in σ is observed for as synthesized CNTs. The dotted line sketches the expected
20 behavior for similar composites prepared from regular, undoped CNTs.

(b) Correspondingly, S steadily decreases with increasing CNT concentration, and crosses over to negative values at $c_s = 40$ wt% CNTs. For higher CNT concentrations, S saturates at about $-10 \mu\text{VK}^{-1}$. For the acid-treated CNTs, S is independent of the
25 CNT concentration in the investigated range. The inset shows the complete measured composition range.

(c) Resulting power factor $S^2\sigma$. For as synthesized CNTs, two regions are apparent, one below c_s , where the composite has p-type properties, and another above c_s , where
30 the material is n-type.

(d) Averaged PL intensity between 675 nm and 725 nm, for samples excited at 514 nm. The inset shows two representative spectra with $c = 0$ wt% and $c = 80$ wt%. Error bars indicate the standard deviation across 2 batches of 6 samples each.

Macroscopically, drop cast films on PET substrates present an electrically percolating behavior as a function of CNT content, with a percolation threshold around $c_p \sim 3.5$ wt% (Figure 8a). This threshold points to relatively well dispersed carbon nanotubes, in agreement with the SEM, AFM, and TXM data shown in Figure 1.

5

To benchmark thermoelectric materials, the dimensionless figure of merit $ZT = S^2\sigma T/\kappa$ is typically used, where S is the Seebeck coefficient ($S > 0$ for p -type and < 0 for n -type semiconductors), σ the electrical conductivity, κ the thermal conductivity, and T the average absolute temperature.

10

The macroscopic σ also increases sharply, in this case by five orders of magnitude, when comparing the neat polymer and composites with weight fractions above percolation. Interestingly, the Seebeck coefficient varies from that of the neat polymer ($\sim 1000 \mu\text{VK}^{-1}$) to that of the CNTs ($\sim -10 \mu\text{VK}^{-1}$) and correlates well with the percolation threshold observed for σ (Figure 8b). Strikingly, at around $c_s \sim 40$ wt% CNT content, the Seebeck coefficient changes sign. The corresponding power factor has two regimes, accordingly, separated by a zero value. Simple modules can be fabricated using these composites, with p - legs with $c=20$ wt%, and n - legs with $c = 80$ wt%. One example consisting of five pairs of such legs is shown in Figure 9 and delivers a thermovoltage of $170 \mu\text{VK}^{-1}$ which is close to the sum of Seebeck coefficients of the constituting legs.

15

20

Since $c_p \ll c_s$, the majority carriers for $c \sim 25$ wt% of CNTs are holes, or, in other words, holes are being transported through the CNTs, which is the electrically more conductive part of the composite. P3HT is effectively doping the CNTs. This is supported by photoluminescence (PL) quenching experiments (Figure 8d), which indicate that there is a strong photoinduced charge transfer between P3HT and CNTs.

25

The observed phenomenology can be well explained in terms of a simple band model, which assumes that the semiconducting CNTs are being co-doped by substitutionally incorporated nitrogen atoms, and P3HT adsorbed on the surface. The Fermi level and the majority charge carrier are then determined by the specific amount of dopants. Furthermore, these composites exhibit thermochromism in solution when heated. Upon increasing the temperature, the composite solution turns from a characteristic dark purple, indicative of π -stacked/crystalline P3HT, to the bright orange coloration associated with well dissolved (amorphous/isolated) P3HT. Unfortunately, this change

30

35

is not preserved through the transition to the dried film, as no changes of the thermoelectric properties are observed. Conversely, a reference P3HT solution does not show any changes during preparation and subsequent heating.

- 5 For samples that were UV-irradiated while drying using a low pressure mercury vapor lamp, the Seebeck coefficient continuously decreases as a function of irradiation time for the investigated samples, which contain 20 wt% and 30 wt% CNTs (Figure 10a). For the 30 wt% samples, S becomes negative after 60s of UV-irradiation.
- 10 In order to understand the impact of UV-irradiation on the thermoelectric properties, we next investigate its effect on the structural and optical properties of the composites.

Optical microscopy indicates that long exposure times (≥ 120 s) yield visibly degraded samples (Figure 11).

15

AFM also suggests an increase in surface roughness (Figure 2), while SEM evidences the appearance of small curled scraps (Figure 1), that are electrically insulating (Figure 6 and 7), which we ascribe to degraded polymer.

- 20 Raman scattering suggests that UV-light has no negative effect on the CNTs (as measured by the ratio of the D and G bands, Figure 12). Overall, long exposure times clearly degrade the samples and as a result, the macroscopic electric conductivity also slightly decreases (Figure 13).

- 25 Figure 10b shows the normalized absorption and PL intensities of four samples irradiated for 0 s, 60 s, 150 s and 240 s. The aforementioned degradation is here seen as an absorption blue-shift, which probably occurs due to a reduction in conjugation length of the polymer. The PL quenching that we discussed before is, upon UV irradiation, much less pronounced, demonstrating a lower degree of charge transfer
- 30 between degraded polymer chains and CNTs, with the concomitant smaller degree of p-doping of the CNTs.

- Figure 10b also shows that there are two clear regimes: for low exposure times (<60 s), there is little degradation of the polymer (no photobleaching, no absorption blue shift,
- 35 high degree of PL quenching) but a strong change in the electronic properties, as

observed by the change in Seebeck sign. Instead, long exposure times (>120 s) result in complete degradation of the polymer with strong negative effects on the electronic properties too. The Fourier transform infrared (FTIR) spectra shown in Figure 14 back up this observation, and provide evidence that the UV treatment attacks both the carbon double bonds of the thiophene ring, as well as the alkyl side chains, influencing the doping not only by reducing conjugation, but also by impairing the CNT-P3HT interaction.

The characteristic peaks of P3HT are related with excitations of the =C-H groups (3055 cm^{-1}), C-H₂ (2924 cm^{-1} , 2856 cm^{-1} , 1454 cm^{-1}), C-H₃ (2954 cm^{-1} , 2870 cm^{-1} , 1377 cm^{-1}) and the C=C thiophene bonds (1560 cm^{-1} , 1512 cm^{-1} , 1460 cm^{-1}). A slight decrease of absorption of these modes is observed with increasing UV treatment time (a, c). This decrease is more pronounced for longer treatment durations (b, c), However an additional effect due to the solvent is then observed.

A thermoelectric module fabricated from a single solution with p- and (UV-irradiated) n-legs was realized. Figure 15 illustrates a proof of concept thermoelectric module and some envisaged applications that are implemented through a toroidal geometry of the module.

The fabrication is detailed in Figure 15. First a uniform wet layer of the composite is deposited on a substrate (s), and part of it is UV-irradiated during drying, resulting in a wet film without treatment (p1) and a wet film that did receive UV treatment (n1). Secondly, the individual legs (p2, n2) of the dried film are patterned by appropriate cutting. We connected p- and n-type legs with an electrical conductor (c) in order to strengthen the bridge region. Then, the device is folded into a spiral, and adjacent couples are connected electrically in series by depositing contacts (c). Lastly, the ends of this spiral are joined to form a torus. Possible applications for this geometry are in the form of a single torus, an extended spiral, and a wristband.

When one side of this module comprising 15 double legs is attached to a glass filled with ice water, leaving the other side at room temperature, it generates a voltage of 5 mV which corresponds to 217.4 $\mu\text{V K}^{-1}$ or 14.5 $\mu\text{V K}^{-1}$ per couple. A plot of the output current and power versus voltage is given in Figure 16. The module supplies ~2 nA at 5 mV Seebeck voltage. An alternative geometry may allow connecting a larger number

of legs to harvest, for instance, waste heat from a pipe. For this, the spiral itself can be wound into yet another spiral.

Importantly, we have measured the bulk thermal conductivity of selected bulk samples and verify that k only slightly increases from $0.29 \text{ Wm}^{-1}\text{K}^{-1}$ for neat P3HT to $0.55 \text{ Wm}^{-1}\text{K}^{-1}$ for a $c = 80 \text{ wt}\%$ composite. (see Table 3). The non-optimized ZT values are then, around 10^{-3} and 10^{-5} for the p-type and n-type composite respectively.

All samples were prepared, measured and stored in atmosphere. Figure 17 shows the results of repeated electrical measurements carried out over a period of up to 600 days. For n-type composites, the conductivity stabilized at 41 % of the initial value, with both high CNT content and UV treated samples following a similar trend. The negative Seebeck coefficient of these samples was stable for every single measured n-type sample, with no significant changes observed after 240 days. In the same amount of time, the Seebeck coefficient of p-type samples diminished to 40 % of the initial value and the electrical conductivity to 11 % of of the initial value.

Table 3. Measured properties used to determine the thermal conductivity κ of bulk P3HT-CNT samples with 13 mm diameter.

	Density ρ [g cm ⁻³]	Specific heat C_p [J kg ⁻¹ K ⁻¹]	Thermal diffusivity α [mm ² s ⁻¹]	Thermal conductivity κ [Wm ⁻¹ K ⁻¹]
pure P3HT	1.05 ± 0.01	1496.79 ± 14.77	0.18 ± 0.00	0.29 ± 0.01
30 wt% CNTs	1.17 ± 0.01	1193.52 ± 2.08	0.35 ± 0.01	0.49 ± 0.02
30 wt% acid-treated CNTs	1.13 ± 0.01	1233.62 ± 3.78	0.29 ± 0.00	0.40 ± 0.03
80 wt% CNTs	1.21 ± 0.01	947.72 ± 1.90	0.48 ± 0.01	0.55 ± 0.04

Example 2: Preparation of a p-type organic semiconductor

SG65i CoMoCAT SWCNTs (SouthWest NanoTechnologies) containing $\approx 40 \%$ (6,5) tubes which are p-type due to doping by atmospheric oxygen, and branched

polyethylenimine (PEI, $M_w \approx 800 \text{ g mol}^{-1}$, $M_w/M_n \approx 1.33$), an electron-rich polymer, were bought from SigmaAldrich.

5 CNTs were dispersed in oDCB at a concentration of 0.5 g L^{-1} and sonicated in ice water for 60 min.

PEI was added in three steps, followed each time by 30 min sonication.

10 The prepared solution was drop-cast onto PET substrates and left to evaporate.

Samples were irradiated for 60 s with 50 mW cm^{-2} of UV-light directly after deposition in a Jelight UVO-Cleaner 42.

15 Fig. 18 shows the measured Seebeck coefficient for samples of different composition, with and without UV-treatment. Concretely, Fig. 18 shows the Seebeck coefficient of composites of single-walled CNTs (which are p-type due to doping with atmospheric oxygen), n-doped with electron-rich PEI.

20 Increasing the concentration of PEI in the composites in all cases reduces the Seebeck coefficient.

n-type samples are obtained for a concentration of PEI greater than 33 wt%.

25 The UV-treatment has the opposite effect, increasing the Seebeck coefficient of all studied samples.

If choosing a suitable composition, it is thus possible to obtain a p-type material by UV-treating an n-type material.

30 In this particular example, this was observed for a composite containing 66 wt% SWCNTs and 33 wt% PEI.

CLAIMS

1. A process of obtainment of an n-type organic semiconductor or a p-type organic semiconductor characterized in that the process comprises the following steps:
- 5 a) preparing a film of a p-type organic semiconductor or a n-type organic semiconductor onto a substrate respectively,
wherein the organic semiconductor comprises a semiconducting nanostructure and an acceptor or donor of electrons respectively; and
- b) irradiating the film obtained in step (a) by UV-VIS radiation with a power between 1
10 mW/cm^2 and $100 \text{ mW}/\text{cm}^2$ and an exposure time of between 0.1 s and 600 s.
2. A process of obtainment of an n-type organic semiconductor according to claim 1, characterized in that the process comprises the following steps:
- a) preparing a film of a p-type organic semiconductor onto a substrate
15 wherein said p-type organic semiconductor comprises
- an n-type semiconducting nanostructure ranging a weight percent between 0.1 % and 60 %; and
 - a p-type semiconducting conjugated molecule;
- and wherein said n-type semiconducting nanostructure is dispersed into the p-
20 type semiconducting conjugated molecule; and
- b) irradiating the film obtained in step (a) by UV-VIS radiation with a power between 1 mW/cm^2 and $100 \text{ mW}/\text{cm}^2$ and an exposure time of between 0.1 s and 600 s.
3. The process according to claim 2, wherein the n-type semiconducting nanostructure
25 of step (a) is selected from the list consisting of N-doped carbon nanotubes, N-doped graphene sheets and graphite nanoplatelets, N-doped graphene nanoribbons, fullerenes, phosphorus doped silicon nanowires, tellurium nanowires such as Bi_2Te_3 nanowires or PbTe nanowires, zinc oxide based nanowires, titanium oxide based nanowires and a combination thereof.
- 30
4. The process according to any of claims 2 or 3, wherein p-type semiconducting conjugated organic molecule of step (a) is selected from polyalkylthiophenes, polyfluorenes, polyaniline, polyacetylene, polyphenylene vinylene, tetracyanoquinodimethane, tetrathiafulvalene and a combination thereof.
- 35

5. The process according to claim 4, wherein the p-type semiconducting conjugated organic molecule of step (a) is poly(3-hexylthiophene), poly(3-dodecylthiophene-2,5-diyl) or poly(9,9-dioctylfluorene).
- 5 6. The process according to any of claims 2 to 5, wherein the n-type semiconducting nanostructure of step (a) ranges a weight percent between 20 % and 40 %.
7. The process according to any of claims 2 to 6, wherein the substrate is flexible and wherein the substrate is selected from polyethylene terephthalate, polyethylene naphthalate, polyimide, polyethylene, polystyrene, poly(vinyl chloride),
10 polytetrafluoroethylene, polypropylene, polyurethane, polyvinylidene fluoride and a combination thereof.
8. The process according to any of claims 2 to 7, wherein step a) comprises the
15 following steps:
- a1) adding a p-type semiconducting conjugated molecule solution comprising a p-type semiconducting conjugated molecule and a solvent to an n-type semiconducting nanostructure dispersion comprising an n-type semiconducting nanostructure and a solvent;
 - 20 a2) agitating the mixture obtained in (a1) at a temperature range between -20 °C and 200 °C; and
 - a3) depositing the solution obtained in step (a2) onto a substrate.
9. The process according to claim 8, wherein step (a2) is performed at a temperature
25 range between 0 °C and 100 °C.
10. The process according to any of claims 8 or 9, characterized in that comprises a step (a1'), between step (a1) and step (a2), of adding a surfactant to the mixture obtained in (a1).
30
11. The process according to any of claims 8 to 10, wherein the wet film obtained in step (a3) has a thickness between 10 μm and 1000 μm,
12. The process according to claim 11, wherein the wet film obtained in step (a3) has a
35 thickness between 100 μm and 1000 μm.

13. The process according to any of claims 1 to 12, wherein step a) comprises the following steps:

- steps (a1) to (a3) according to any of claims 7 or 8; and
5 a step (a4) of drying the wet film obtained in step (a3) by evaporating the solvents.

14. The process according to claim 13, wherein the dried film obtained in step (a4) has a thickness between 10 nm and 100 μm ,

10

15. The process according to claim 14, wherein the dried film obtained in step (a) has a thickness between 1 μm and 10 μm .

16. The process of obtainment of a p-type organic semiconductor according to claim 1, characterized in that the process comprises the following steps:

15

a) preparing a film of a n-type organic semiconductor onto a substrate

wherein said n-type organic semiconductor comprises

- a p-type semiconducting nanostructure ranging a weight percent between 0.1 % and 80 %; and
- 20 • an electron-rich molecule;

and wherein said p-type semiconducting nanostructure is dispersed into the electron-rich molecule; and

b) irradiating the film obtained in step (a) by UV-VIS radiation with a power between 1 mW/cm^2 and 100 mW/cm^2 and an exposure time of between 0.1 s and 600 s.

25

17. The process according to claim 16, wherein the p-type semiconducting nanostructure of step (a) are pristine single-double- and multi-walled carbon nanotubes, graphene sheets and graphite nanoplatelets, graphene nanoribbons; boron doped single- double- and multi-walled carbon nanotubes, boron doped graphene sheets and boron doped graphite nanoplatelets, boron doped graphene nanoribbons, boron doped fullerenes and a combination thereof

30

18. The process according to any of claims 16 or 17, wherein the electron-rich molecule of step (a) is selected from polyethylenimine (PEI), diethylenetriamine (DETA), tetramethylammonium hydroxide (TMAH), tetrakis(dimethylamino)ethylene

35

(TDAE), 4-*H*-benzimidazol-2-yl)-*N,N*-dimethylbenzenamine (N-DMBI), 4-*H-N,N*-diphenylaniline (N-DPBI), triphenylphosphine (tpp), 1,3-bis(diphenylphosphino)propane (dppp)..

5 19. The process according to any of claims 16 to 18, wherein the p-type semiconducting nanostructure of step (a) ranges a weight percent between 40 % and 80 %.

10 20. The process according to any of claims 16 to 19, wherein the substrate is flexible and wherein the substrate is selected from polyethylene terephthalate, polyethylene naphthalate, polyimide, polyethylene, polystyrene, poly(vinyl chloride), polytetrafluoroethylene, polypropylene, polyurethane, polyvinylidene fluoride and a combination thereof.

15 21. The process according to any of claims 1 to 20, wherein step (b) is performed by UV-VIS radiation with a power between 40 mW/cm² and 60 mW/cm² and an exposure time of between 50 s and 100 s.

20 22. The process according to any of claims 1 to 21, wherein step (b) is performed in the presence of an oxygen containing atmosphere.

23. The process according to any of claims 1 to 22, wherein step (b) is performed using a laser source, a diode or a lamp.

Fig 1.

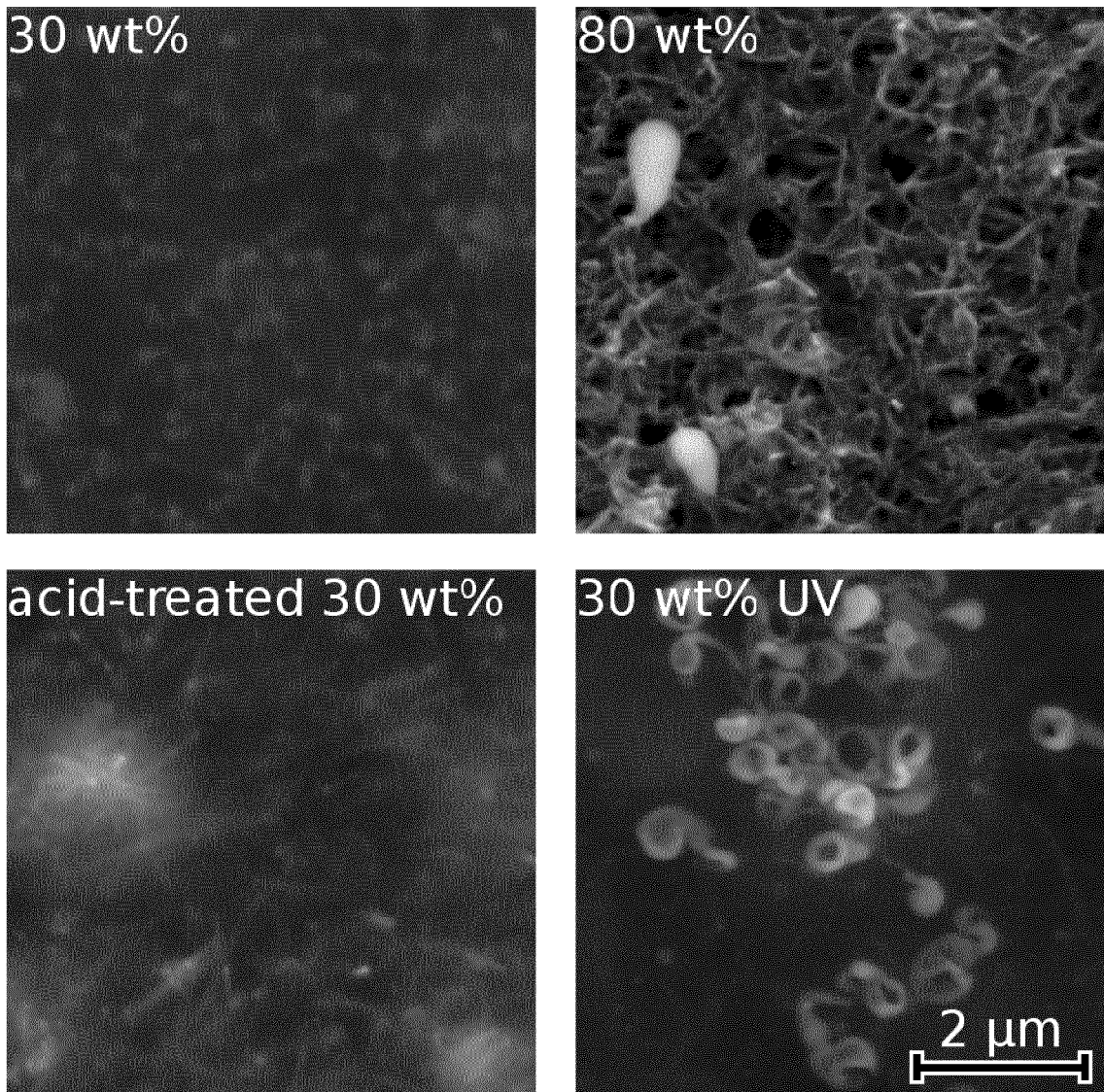


Fig 2.

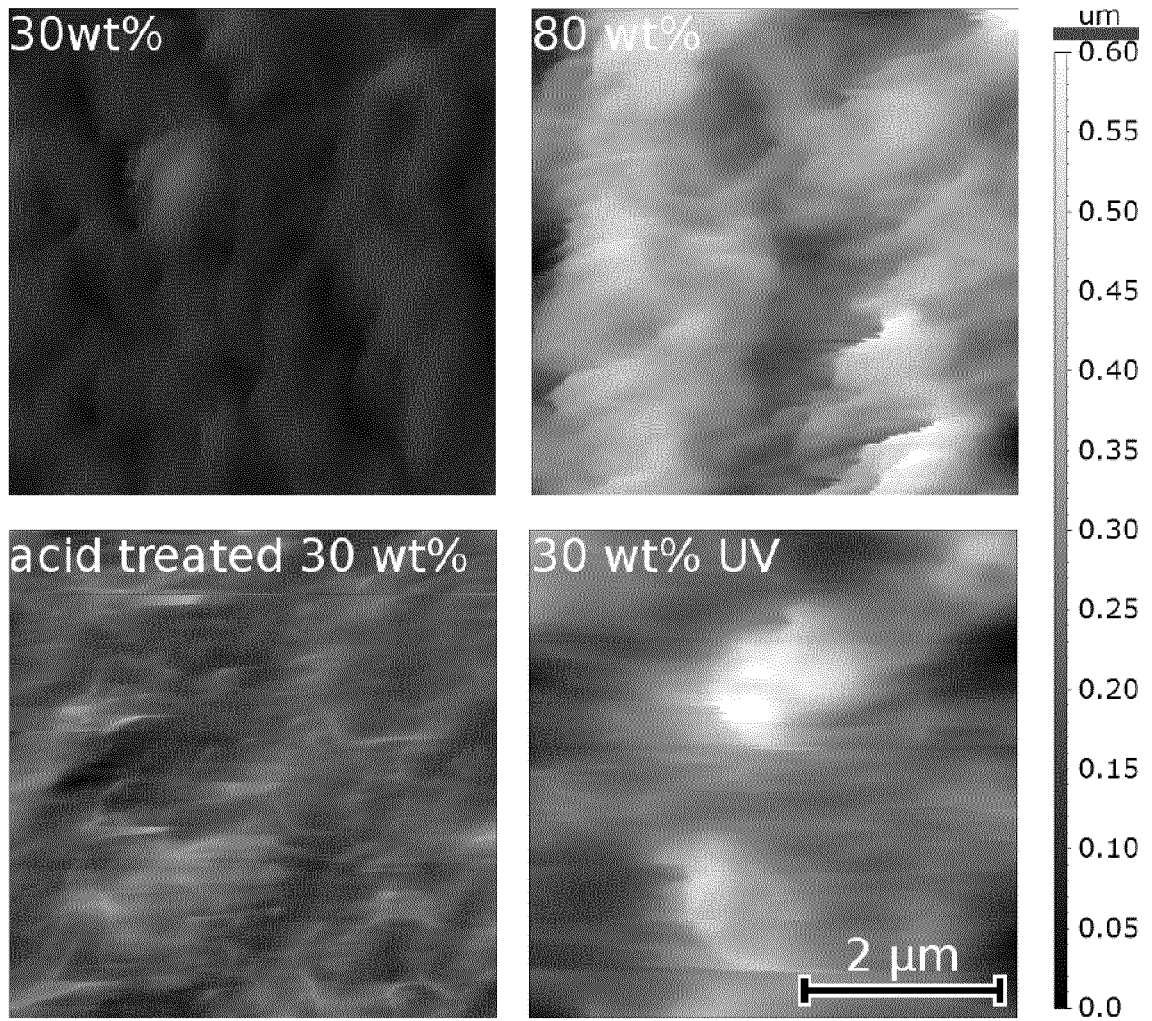


Fig. 3
399 eV

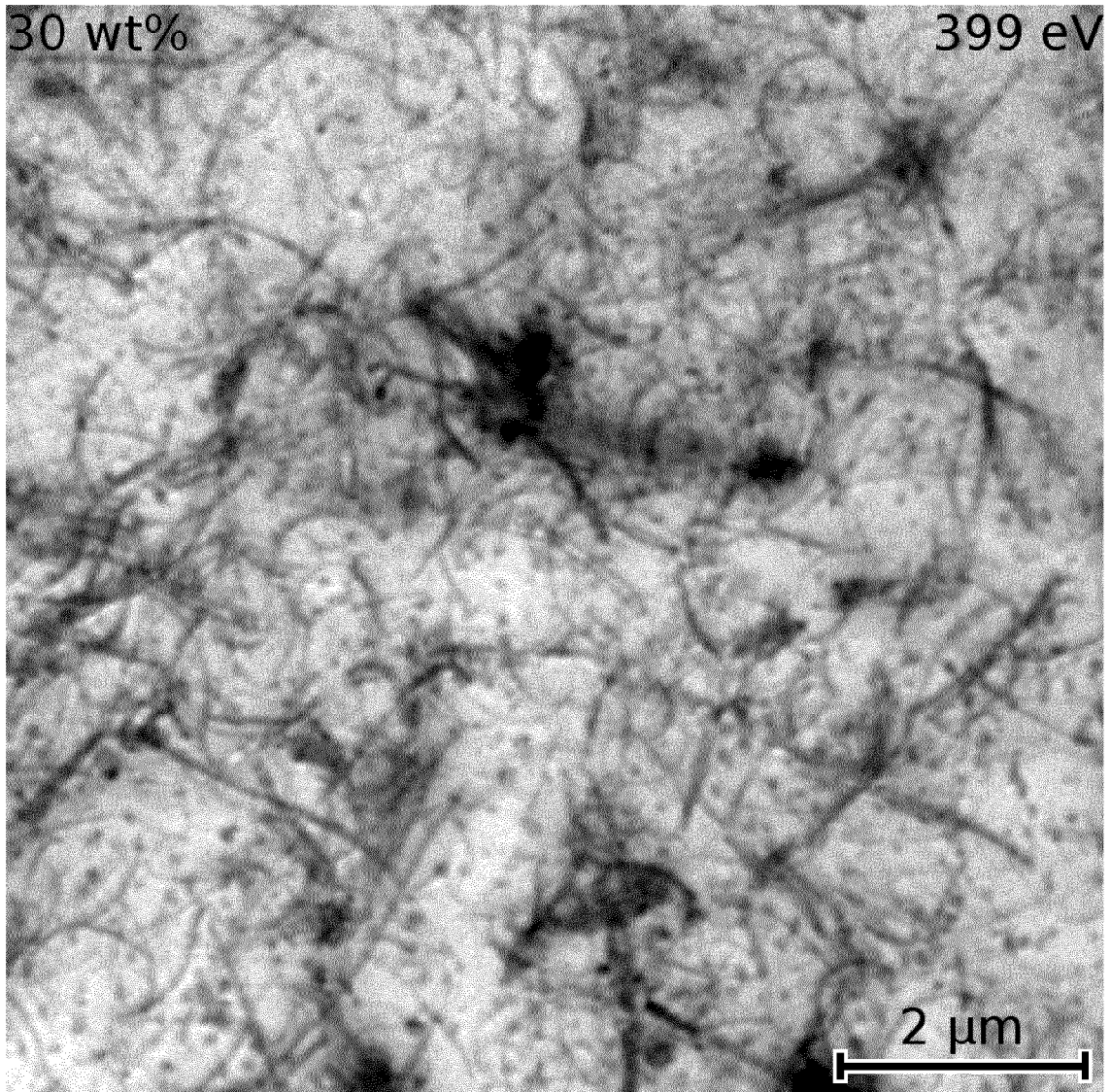


Fig. 4
520eV

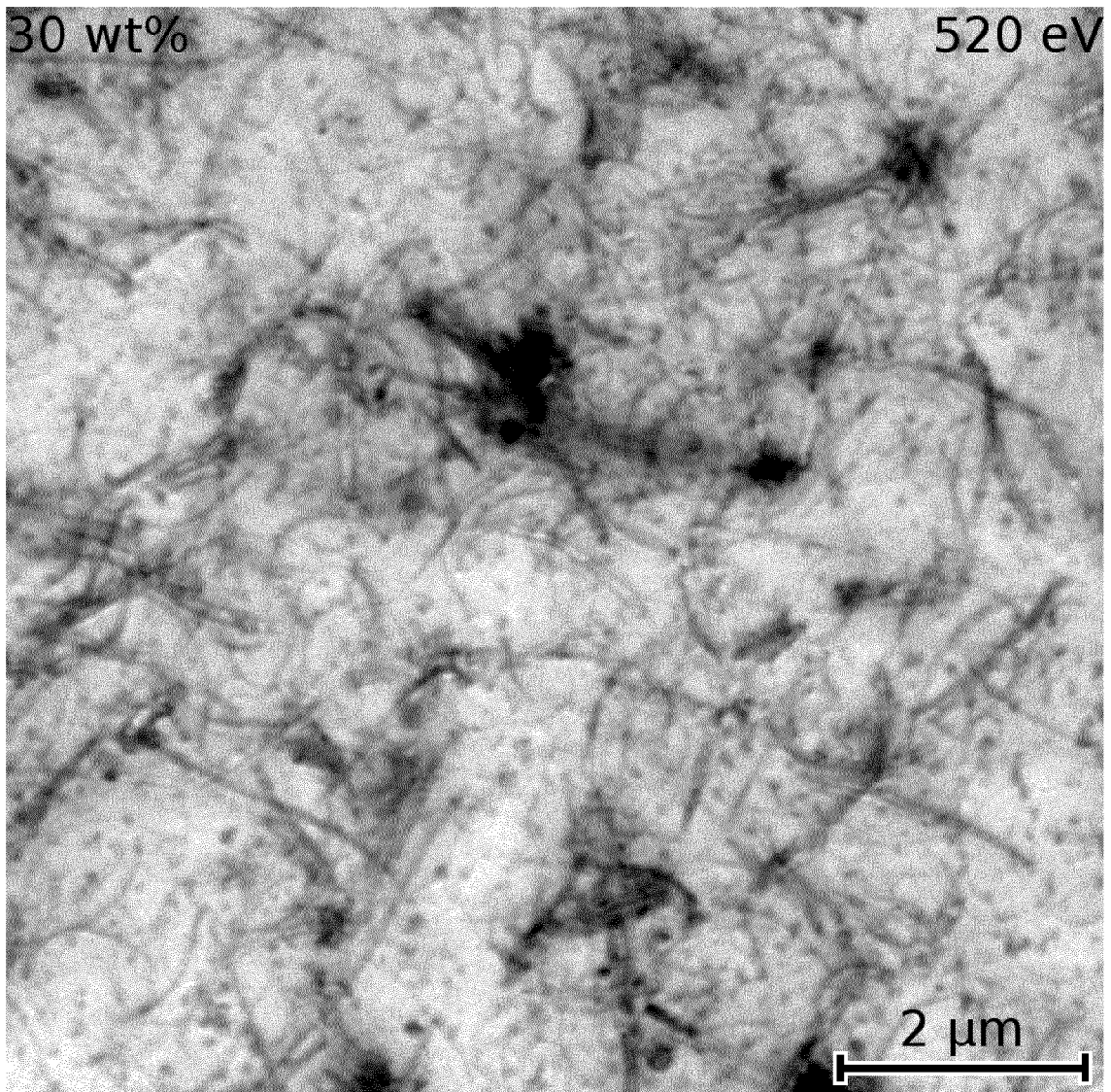


Fig. 5
707eV iron

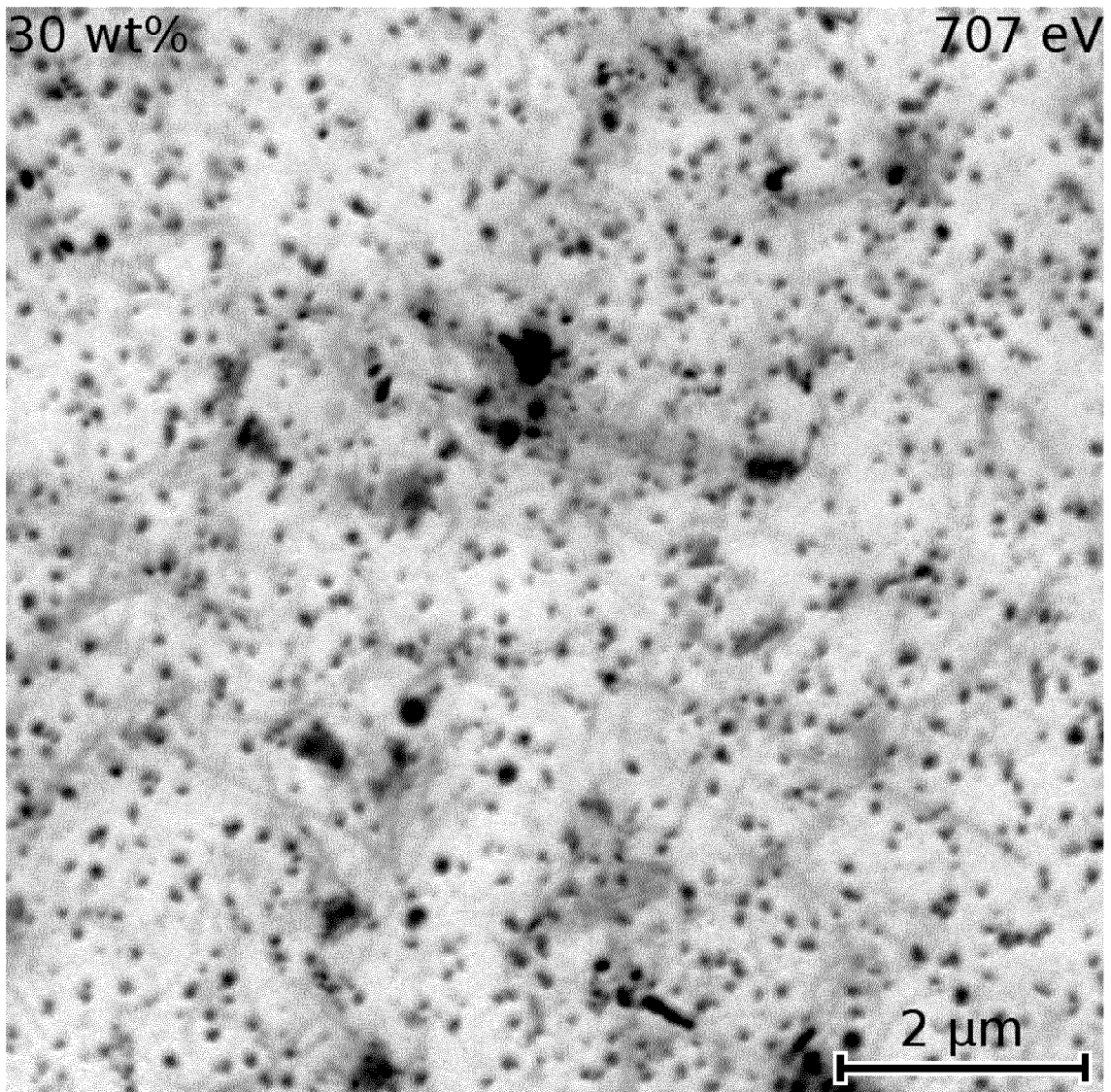


Fig. 6

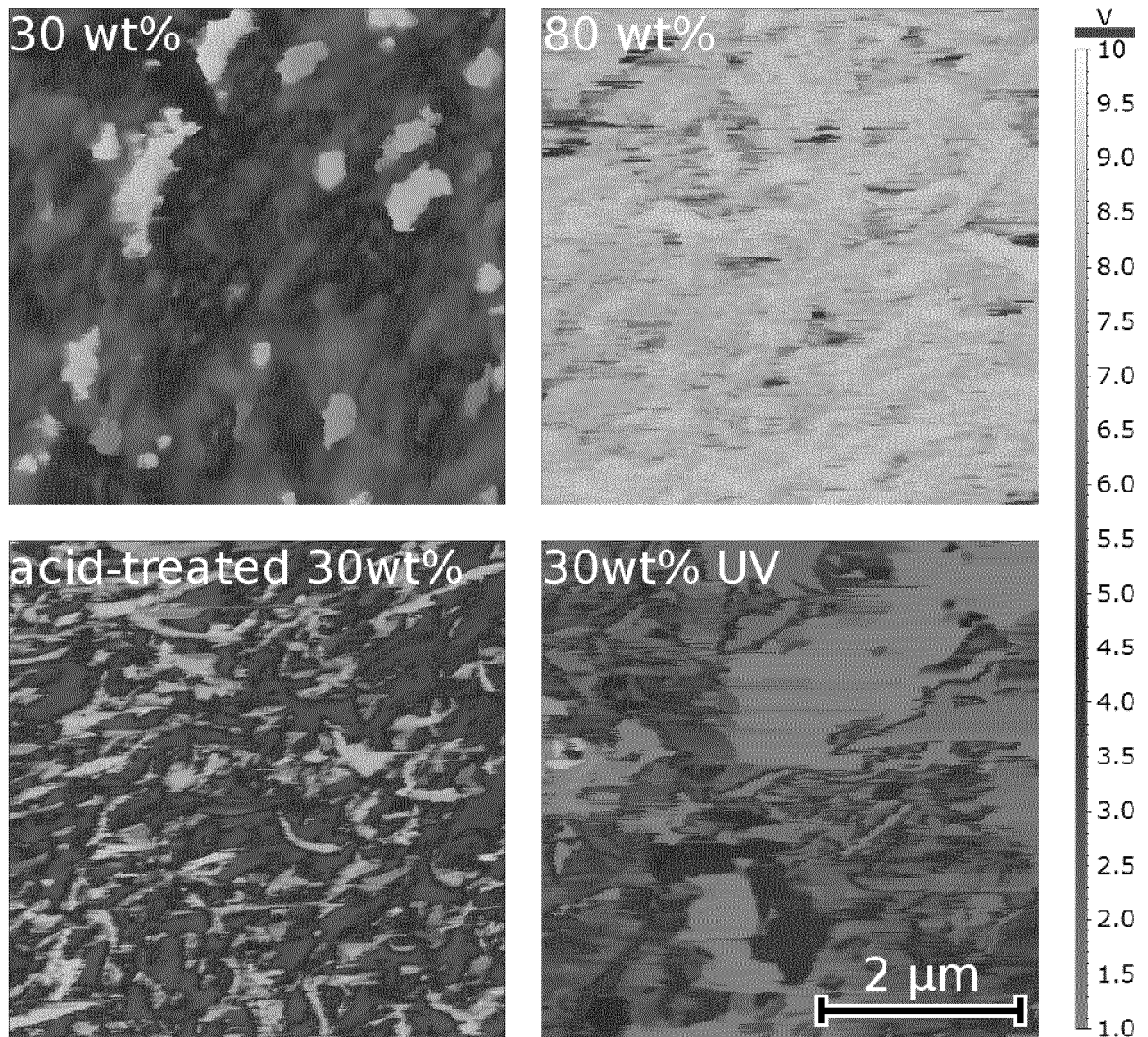


FIG. 7

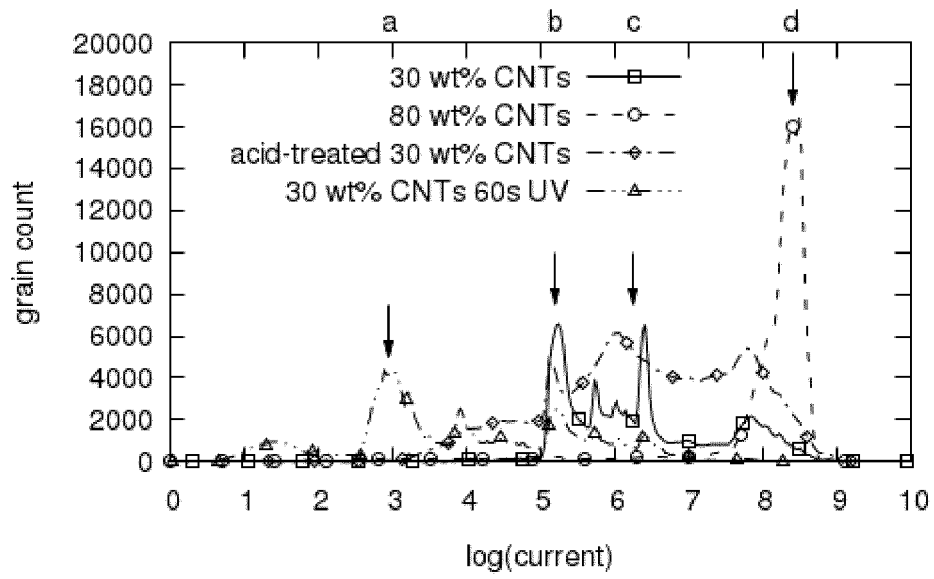


FIG. 8

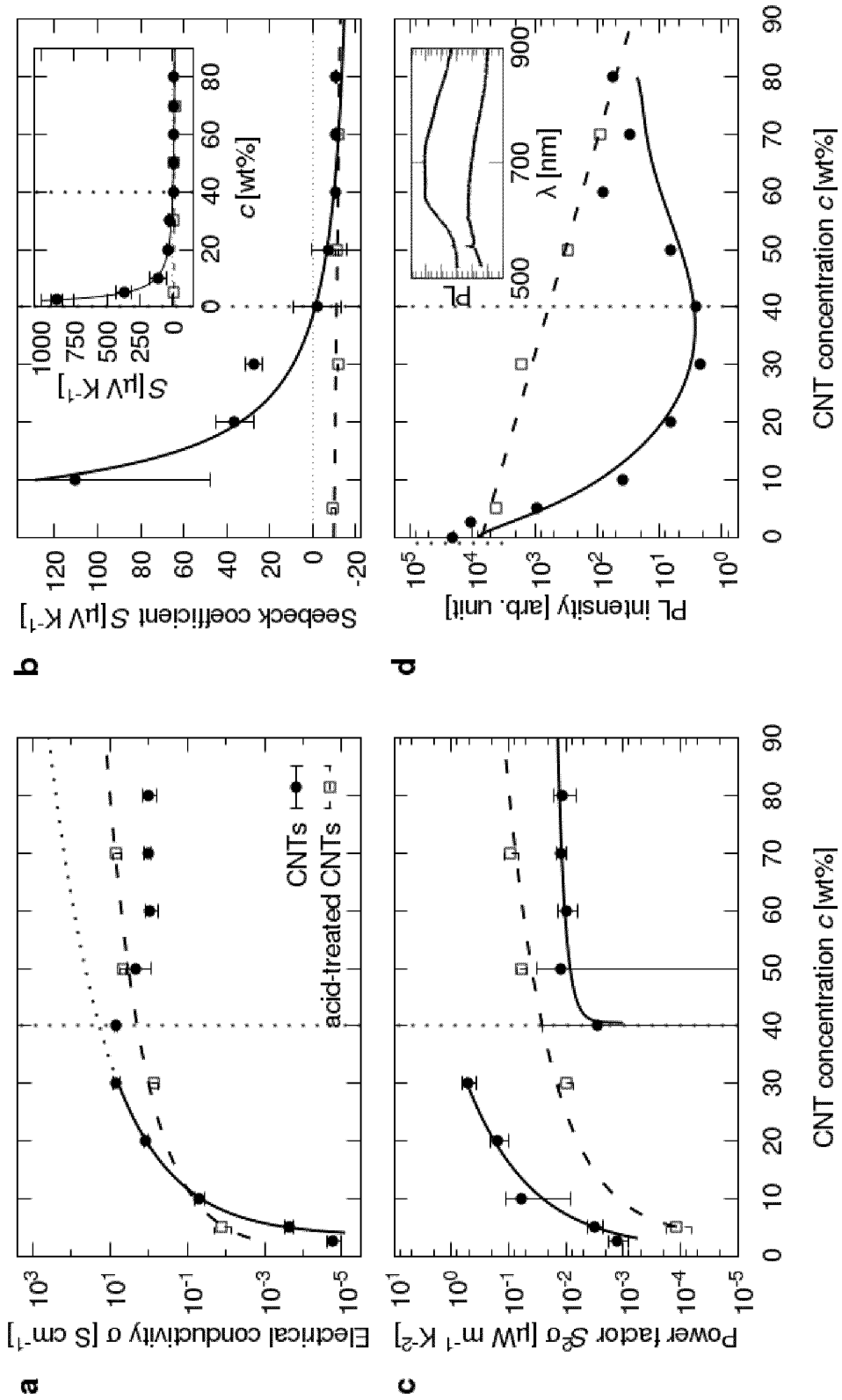


FIG. 9

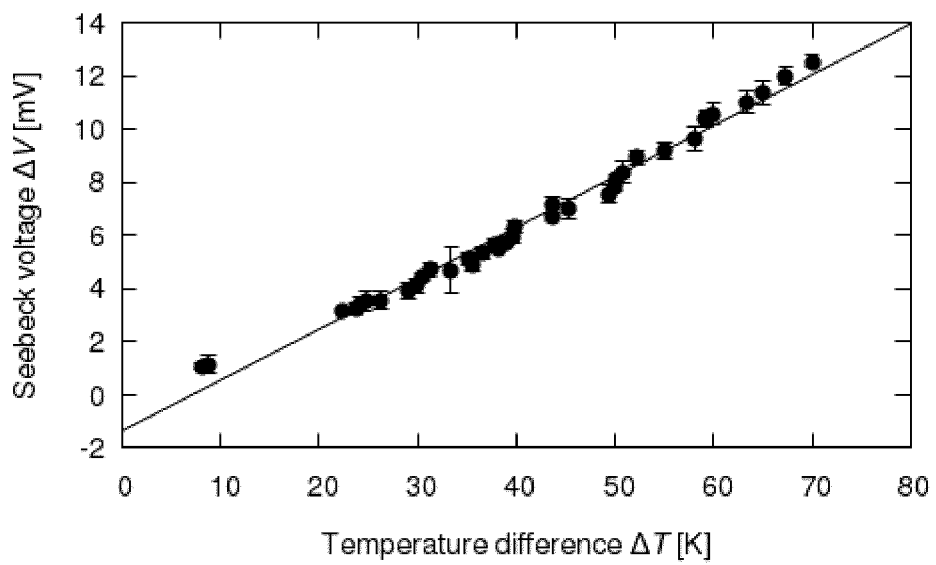
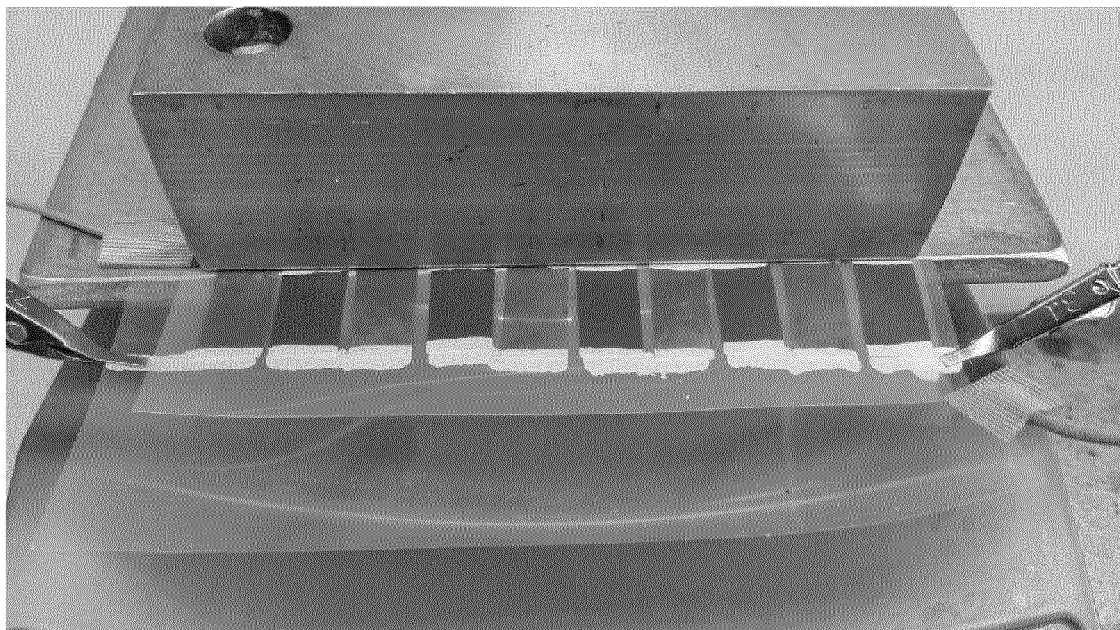


FIG. 10

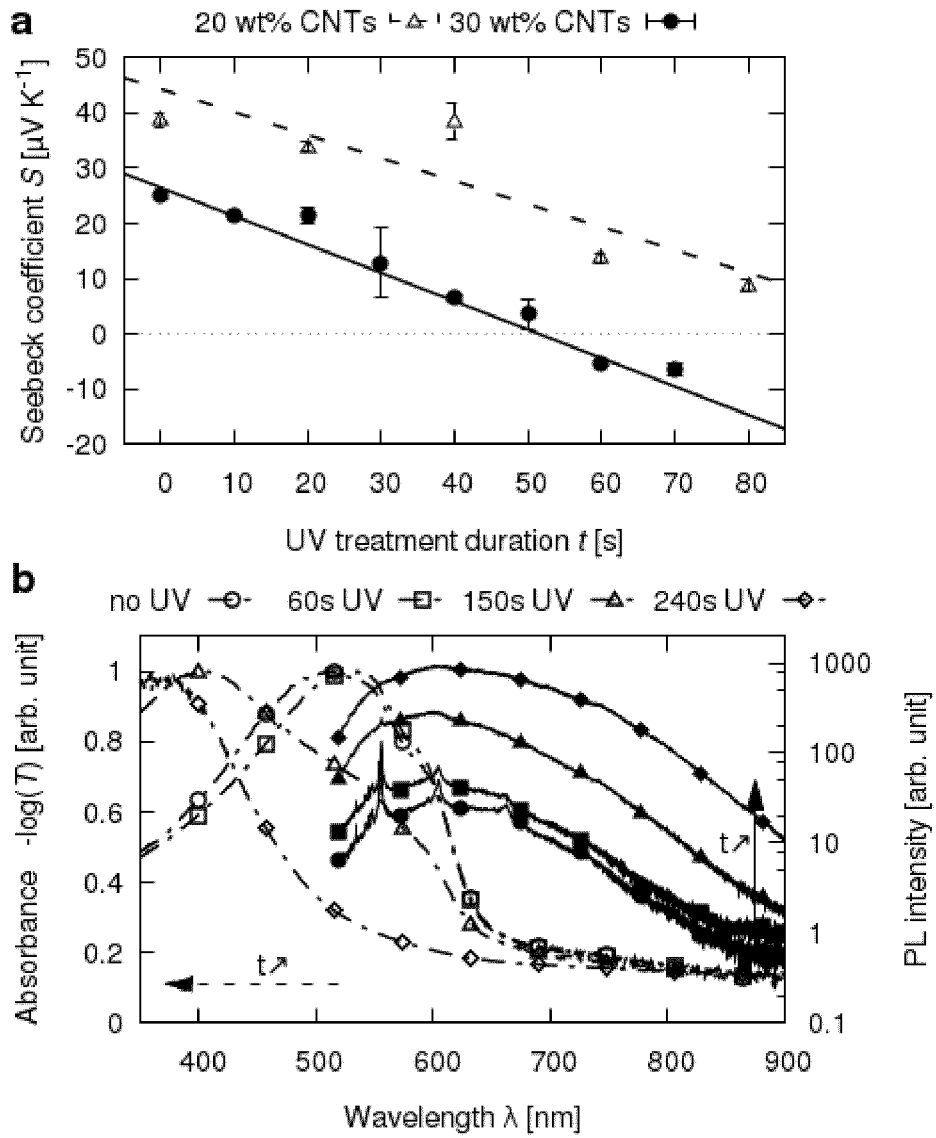


FIG. 11

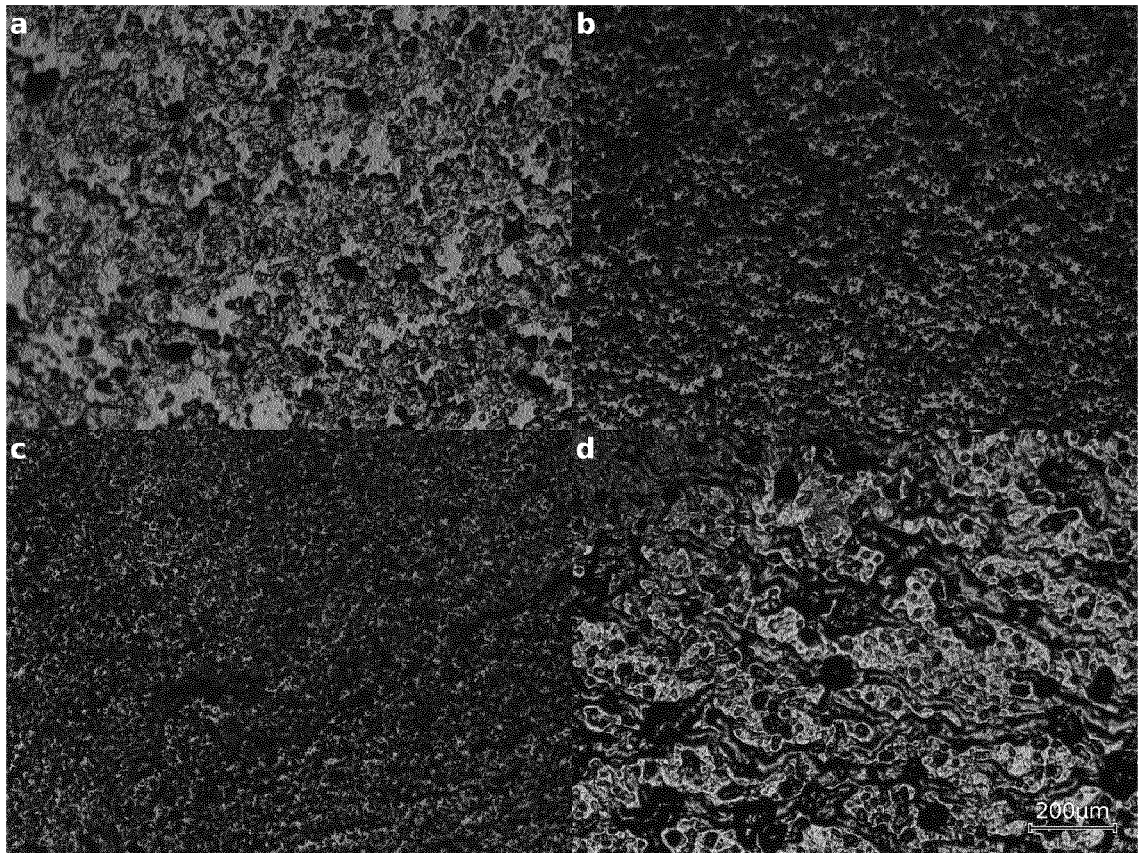


FIG. 12

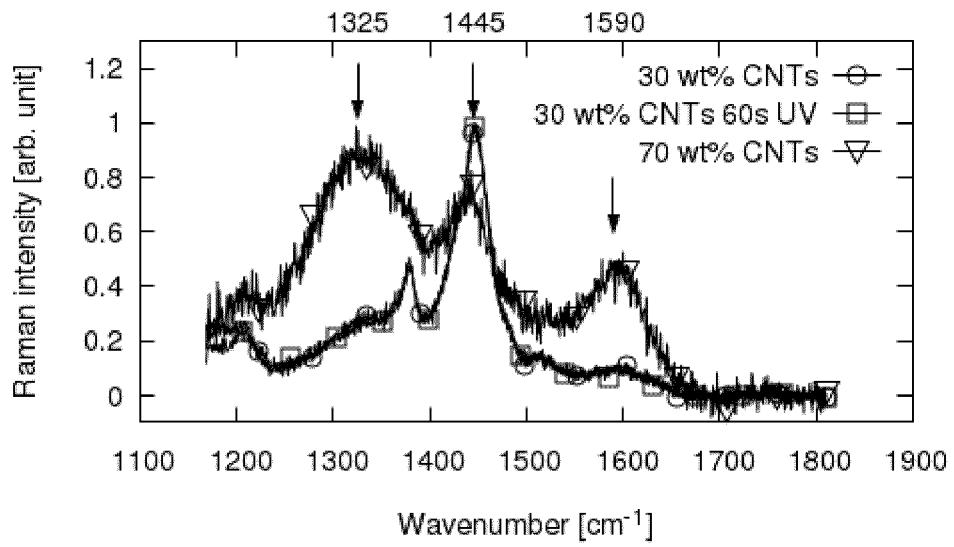


FIG. 13

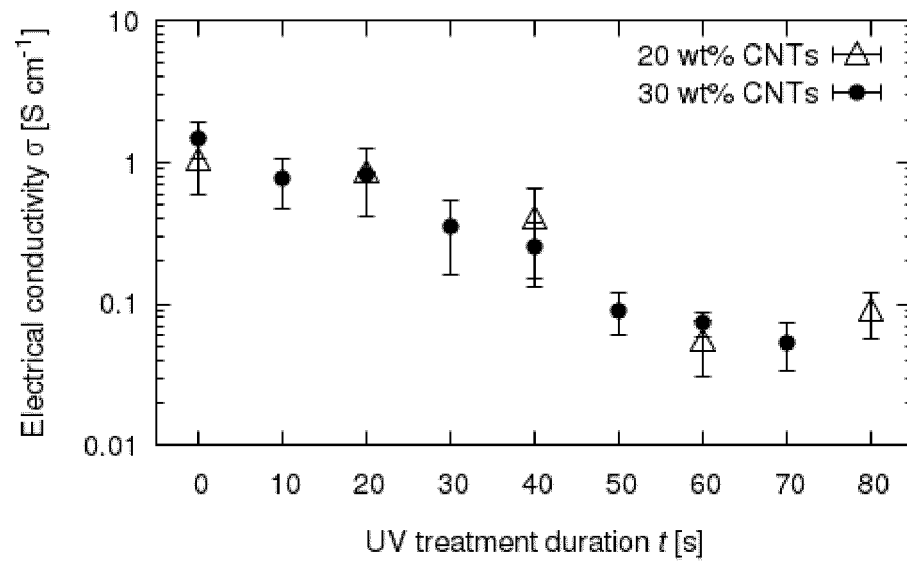


FIG. 14

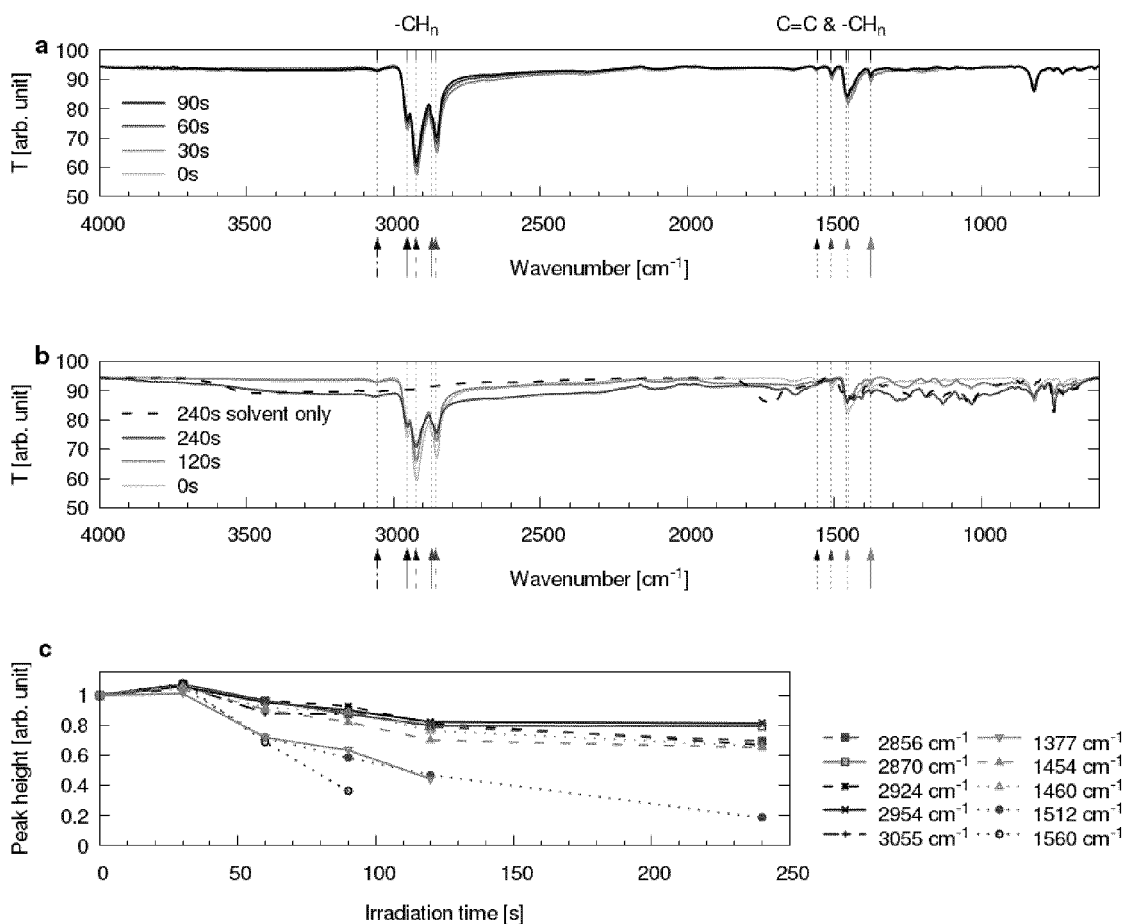


FIG. 15

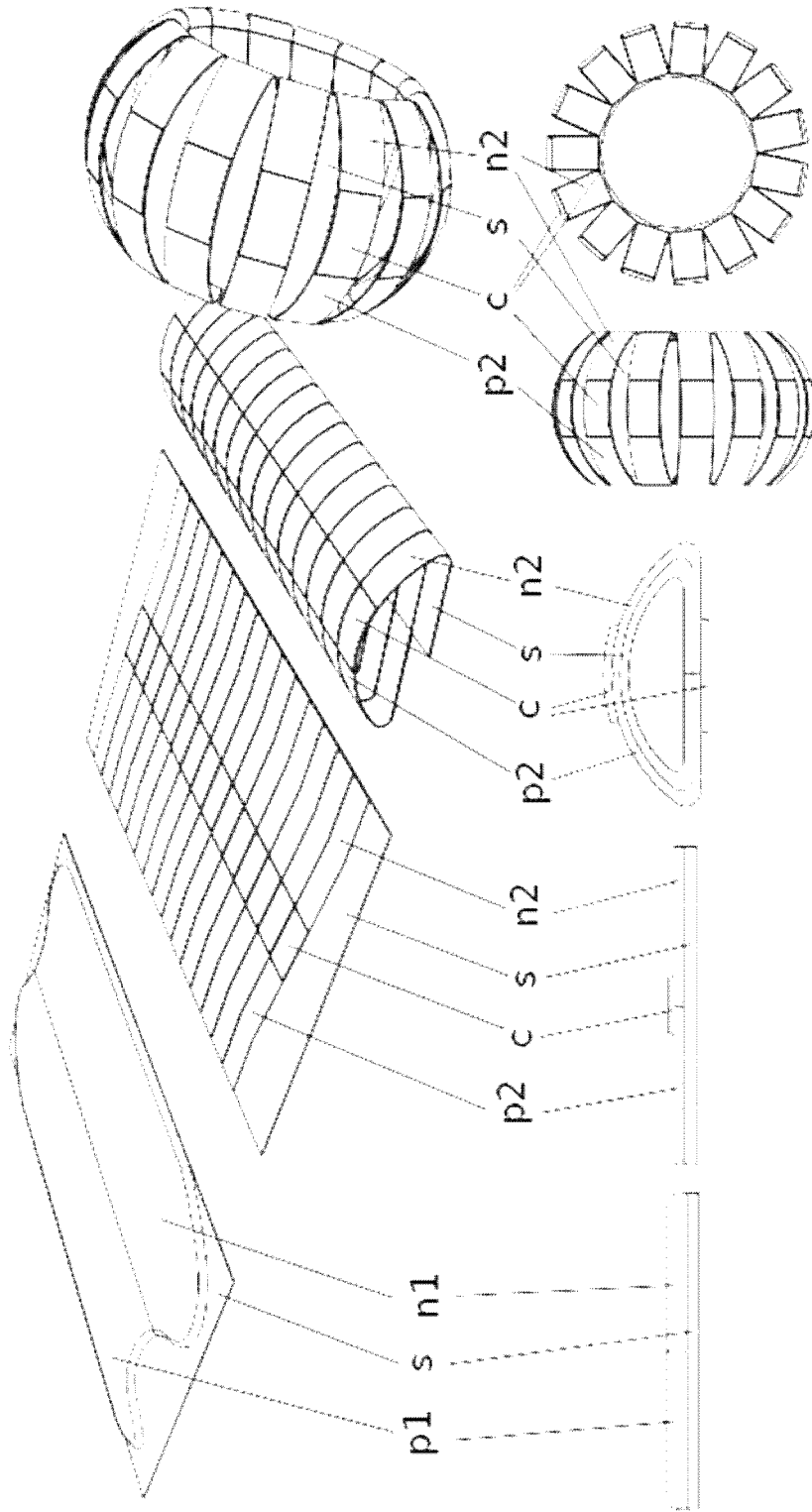


FIG 16.

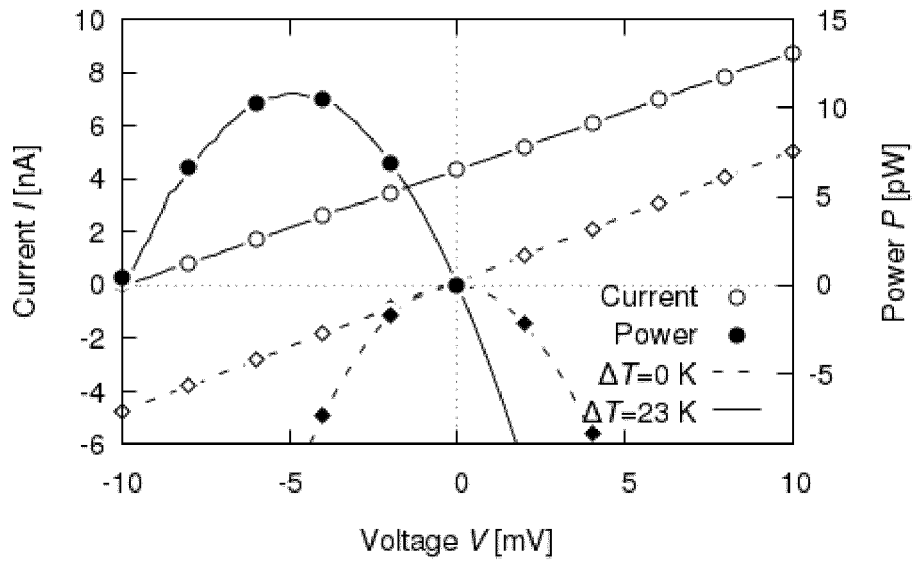


FIG. 17

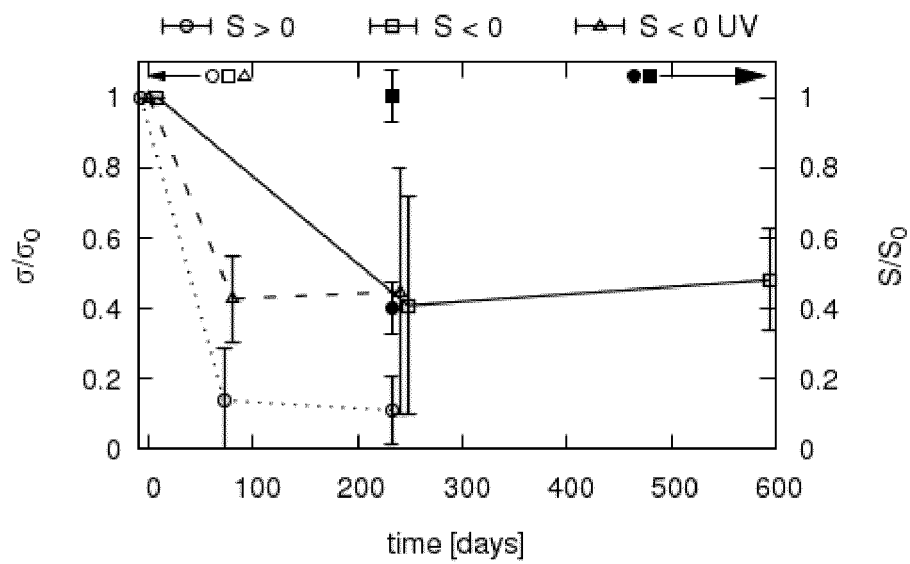
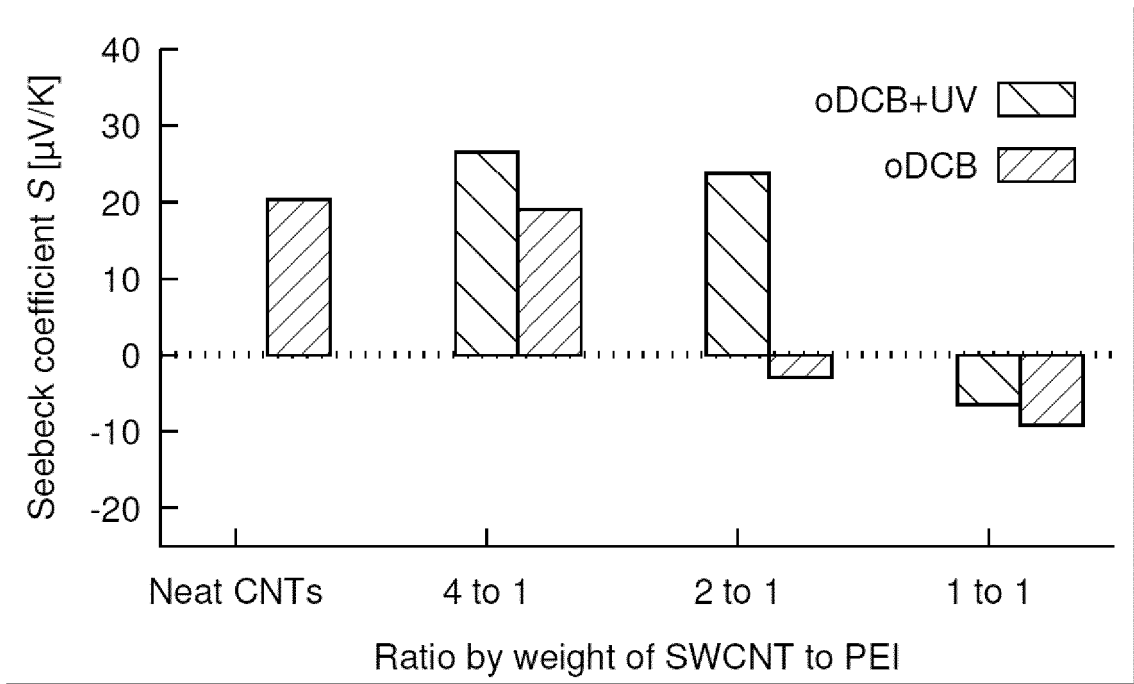


FIG. 18



INTERNATIONAL SEARCH REPORT

International application No
PCT/EP2016/078459

A. CLASSIFICATION OF SUBJECT MATTER
INV. H01L51/00
ADD.
According to International Patent Classification (IPC) or to both national classification and IPC

B. FIELDS SEARCHED
Minimum documentation searched (classification system followed by classification symbols)
H01L

Documentation searched other than minimum documentation to the extent that such documents are included in the fields searched

Electronic data base consulted during the international search (name of data base and, where practicable, search terms used)
EPO-Internal

C. DOCUMENTS CONSIDERED TO BE RELEVANT

Category*	Citation of document, with indication, where appropriate, of the relevant passages	Relevant to claim No.
X	SHIM M ET AL: "PHOTOINDUCED CONDUCTIVITY CHANGES IN CARBON NANOTUBE TRANSISTORS", APPLIED PHYSICS LETTERS, A I P PUBLISHING LLC, US, vol. 83, no. 17, 27 October 2003 (2003-10-27), pages 3564-3566, XP001192562, ISSN: 0003-6951, DOI: 10.1063/1.1622450	1,21,23
A	page 3564, column 1, paragraph 3 - page 3565, column 1, paragraph 2; figure 1 ----- -/--	2-20,22

Further documents are listed in the continuation of Box C.

See patent family annex.

* Special categories of cited documents :

- "A" document defining the general state of the art which is not considered to be of particular relevance
- "E" earlier application or patent but published on or after the international filing date
- "L" document which may throw doubts on priority claim(s) or which is cited to establish the publication date of another citation or other special reason (as specified)
- "O" document referring to an oral disclosure, use, exhibition or other means
- "P" document published prior to the international filing date but later than the priority date claimed

- "T" later document published after the international filing date or priority date and not in conflict with the application but cited to understand the principle or theory underlying the invention
- "X" document of particular relevance; the claimed invention cannot be considered novel or cannot be considered to involve an inventive step when the document is taken alone
- "Y" document of particular relevance; the claimed invention cannot be considered to involve an inventive step when the document is combined with one or more other such documents, such combination being obvious to a person skilled in the art
- "&" document member of the same patent family

Date of the actual completion of the international search 10 February 2017	Date of mailing of the international search report 07/03/2017
Name and mailing address of the ISA/ European Patent Office, P.B. 5818 Patentlaan 2 NL - 2280 HV Rijswijk Tel. (+31-70) 340-2040, Fax: (+31-70) 340-3016	Authorized officer Bakos, Tamás

INTERNATIONAL SEARCH REPORT

International application No
PCT/EP2016/078459

C(Continuation). DOCUMENTS CONSIDERED TO BE RELEVANT		
Category*	Citation of document, with indication, where appropriate, of the relevant passages	Relevant to claim No.
A	<p>CHEON TAEK HONG ET AL: "Spray-printed CNT/P3HT organic thermoelectric films and power generators", JOURNAL OF MATERIALS CHEMISTRY A: MATERIALS FOR ENERGY AND SUSTAINABILITY, vol. 3, no. 43, 5 October 2015 (2015-10-05), pages 21428-21433, XP055344634, GB ISSN: 2050-7488, DOI: 10.1039/C5TA06096F the whole document</p> <p style="text-align: center;">-----</p>	1-15
A	<p>YEONTACK RYU ET AL: "High electrical conductivity and-type thermopower from double-/single-wall carbon nanotubes by manipulating charge interactions between nanotubes and organic/inorganic nanomaterials", CARBON, ELSEVIER, OXFORD, GB, vol. 49, no. 14, 29 June 2011 (2011-06-29), pages 4745-4751, XP028264443, ISSN: 0008-6223, DOI: 10.1016/J.CARBON.2011.06.082 [retrieved on 2011-06-29] the whole document</p> <p style="text-align: center;">-----</p>	16-20